LBNL-41278

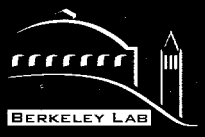

ERNEST ORLANDO LAWRENCE
BERKELEY NATIONAL LABORATORY

Sorbent-Coated Diffusion Denuders for Direct Measurement of Gas/Particle Partitioning by Semi-Volatile Organic Compounds

Lara A. Gundel and Douglas A. Lane

Environmental Energy Technologies Division

January 1998

LBNL-41278
UC-000

SORBENT-COATED DIFFUSION DENUDERS FOR DIRECT MEASUREMENT OF GAS/PARTICLE PARTITIONING BY SEMI-VOLATILE ORGANIC COMPOUNDS

Lara A. Gundel
Ernest Orlando Lawrence Berkeley National Laboratory
University of California
One Cyclotron Road
Berkeley, CA 94720, USA

and

Douglas A. Lane
Atmospheric Environment Service
4905 Dufferin Street
North York, ON, M3H 5T4, Canada

January 1998

This work was supported by Grant number 5-R01-HL42490 from the National Heart Lung and Blood Institute, Public Health Service, Department of Health and Human Services, by the Energy Research Laboratory Technology Research Program of the U. S. Department of Energy, by the Atmospheric Research and Exposure Assessment Laboratory, Office of Research and Development, U. S. Environmental Protection Agency, through the U. S. Department of Energy, under Contract No. DE-AC03-76SF00098, and by the Atmospheric Environment Service of Environment Canada.

Table of Contents

1. INTRODUCTION
   - 1.1 Significance 3
   - 1.2. The Need for Improved Measurements of Semi-volatile Organic Species 3
   - 1.3. Diffusion-Based Sampling for Semi-Volatile Organic Species 4
   - 1.4. Overview ..... 4 - 5
2. DIRECT DETERMINATION OF SVOC WITH SORBENT-COATED ANNULAR DENUDERS 5
   - 2.1. Extractable Coatings for Diffusion Denuders 5
   - 2.2. Styrene-Divinylbenzene Polymer Resins for Air Sampling ..... 5 - 6
   - 2.3 Denuder Fluid Dynamics and Efficiency ..... 6 - 7
3. THE INTEGRATED ORGANIC VAPOR/PARTICLE SAMPLER (IOVPS) 7
   - 3.1. Design ..... 7 - 8
   - 3.2. Performance Validation 8
     - 3.2.1. Collection Efficiency ..... 8 - 10
     - 3.2.2. Capacity ..... 10 - 11
     - 3.2.3. Particle Transmission Through the IOVPS 11
     - 3.2.4. Comparison to Filter-Sorbent Bed Sampling ..... 12 - 13
     - 3.2.5. Sampling Artifacts ..... 13 - 14
   - 3.3. Phase Distributions of Ambient PAH in Berkeley, CA ..... 14 - 15
   - 3.4. Phase Distributions of PAH in Environmental Tobacco Smoke ..... 15 - 16
   - 3.5. Phase Distributions of Nicotine in Environmental Tobacco Smoke 16
   - 3.6 The IOVPS in Other Applications 16
     - 3.6.1. Kinetics of the Formation and Decay of Nitro-PAH ..... 16 - 17
     - 3.6.2. Atmospheric Behavior of Dioxins 17
     - 3.6.3. Kinetics and Thermodynamics of Gas/Particle Partitioning ..... 17 - 18
     - 3.6.4. Semi-Volatile Organic Compounds from Combustion Sources 18
     - 3.6.5. Semi-Volatile Organic Compounds in Secondary Aerosols 18
4. THE INTEGRATED ORGANIC GAS AND PARTICLE SAMPLER (IOGAPS) ..... 18 - 19
   - 4.1. The Prototype IOVPS-GAP Hybrid Sampler 19
     - 4.1.1 Polycyclic Aromatic Hydrocarbons in Berkeley, CA ..... 19 - 20
     - 4.1.2. Comparison to IOVPS 20
   - 4.3. Design Parameters for the IOGAPS ..... 20 - 21
   - 4.4. Jumbo-IOGAPS 21
5. SUMMARY AND CONCLUSIONS 22
6 ACKNOWLEDGEMENTS 23
7. REFERENCES ..... 24 - 26
8. TABLES 27
9 FIGURES ..... 27 - 28

1. INTRODUCTION

1.1. Significance

Many environmentally-persistent chemical pollutants are semi-volatile organic compounds (SVOC) (such as polycyclic aromatic hydrocarbons and pesticides) that enter the base of the food chain through pathways that depend initially on their phase distributions in the atmosphere. Many of these SVOC have been shown to have potential for reproductive and endocrine disrupting effects [1].

The environmental fates of semi-volatile organic species are phase dependent because atmospheric reactions and transport and deposition processes differ for gaseous and particulate semi-volatile species [2]. For example, for many SVOC, the nature and extent of contaminant transport from air to surface water [3] or from air to vegetation and into food chains [4] are very strongly dependent on partitioning between the gas and particle phases in the atmosphere. Whether intermedia transport takes place in the gas or particulate phase can have a strong impact on the estimated extent of human and ecosystem exposures. In addition, health effects due to exposure to toxic air pollutants are phase dependent since lung deposition patterns differ between the gas and particulate phases [5]. Furthermore, strategies to control semi-volatile organic environmental pollutants require information on phase distributions [6].

Efforts to move from the existing qualitative characterization of the importance of partitioning of SVOC to more quantitative characterization have been hindered by a number of scientific obstacles. One major problem is the quality of many of the measurements of the partitioning of these chemicals between the gas phase and airborne particulate matter, between the gas phase and soils, and between the gas phase and vegetation. For example, most existing measurements of vapor-particle partitioning are suspected to show large artifacts (biases) due to the sampling methods used. An additional problem is the lack of a modeling framework that includes coupled mass exchange at multiple media boundaries (soil, air, vegetation, etc.), and that appropriately links the space and time scales involved in long-range transport when multiple media are integrated [7].

1.2. The Need for Improved Measurements of SVOC

Most phase distribution measurements worldwide have been made by determining the concentrations of particulate-phase semi-volatile organic species from filters that are followed by adsorbents ("conventional samplers"). The material retained by the adsorbents is interpreted as yielding the gas phase concentrations. Since sorbent beds follow filters, desorption of semi-volatile compounds from the particles on the filters, *i.e.*, negative particulate-phase artifacts (with subsequent trapping on the sorbents) or adsorption of gases by the filter materials, *i.e.*, positive particulate-phase artifacts, can lead to incorrect measurements of gas and particulate-phase concentrations. The errors depend on pollutant volatility and the sorption characteristics of the particles, as well as the type of filter material, temperature and the sampling rate and temperature. Many existing atmospheric measurements of semi-volatile polycyclic aromatic hydrocarbons (PAH), pesticides, dioxins and PCBs are thought to be significantly biased by negative particulate-phase artifacts that may overestimate, by up to an order of magnitude, the gas phase concentrations of these SVOC [2].

1.3. Diffusion-Based Sampling for Semi-volatile Organic Species

In contrast, diffusion denuder technology provides a less artifact-encumbered approach for accurate determination of phase distributions of semi-volatile species because the gas phase is collected before the particulate phase. Large particles are removed from the airstream by a size-selective inlet followed by a coated denuder surface that collects and retains gas-phase species that diffuse from the moving airstream to the coating. The surface does not influence particle transport to a downstream filter. A sorbent or denuder placed after the filter traps any material desorbed from the particles after they are collected on the filter.

Diffusion-based measurements have been incorporated into several studies that used two or more co-located sampling trains (conventional and diffusion-based) to investigate phase distributions of SVOC (hexachlorocyclohexane pesticides, [8,9]; polycyclic aromatic hydrocarbons, [10,11]; carbonaceous SVOC, [12,13]). These samplers did not measure the gas phase concentrations directly, but rather as the difference between the conventional side (filter plus sorbent) and denuded airstream (filter plus sorbent). However, since the difference-based methods required paired samplers, the costs were high, and quality of the results may have suffered because of the large number of sources of error, compared to direct determination of the gas phase.

1.4. Overview

This chapter describes Lawrence Berkeley National Laboratory's new diffusion-based sampling approach for semi-volatile organic species that allows direct determination of both the gas and particulate phases [14]. Here, the gas phase species are extracted from collection surfaces that have a high-purity adsorbent resin coating. Extracts of filters and sorbents are then quantitated by the same analytical schemes as used for conventional samplers. The first such sampler, the Integrated Organic Vapor/Particle Sampler (IOVPS), was developed and validated at Lawrence Berkeley National Laboratory to investigate phase distributions of PAH and nicotine in environmental tobacco smoke (ETS) and indoor air [14,15]. Its denuder sections have the same dimensions as currently used for sampling acid gases in ambient air [16]. In a single-channel version, its sampling capacity for ambient air is limited to about 2 m^3. For higher capacity, other investigators have used multi-channel versions of the IOVPS (with longer tubes), for investigation of the formation and decay of nitro-PAH [17-20], kinetics of gas/particle partitioning of PAH [21-24] and phase distribution measurements of a range of semi-volatile organics in a variety of combustion sources [25,26]. Currently the IOVPS is also part of investigations of gas/particle partitioning of chamber-generated smog [27].

The chapter also describes new higher capacity samplers that can be used at higher flow rates and longer collection periods in ambient air. A collaboration between investigators at LBNL and the Atmospheric Environment Service of Environment Canada has produced diffusion-based samplers that incorporate the IOVPS coating on the diffusion denuder surfaces of the Gas and Particle (GAP) sampler [8]. The first hybrid Integrated Organic Gas and Particle Sampler (IOGAPS) sampled PAH in ambient air at 16.7 L min^{-1} for 24 hours in Berkeley, CA in April 1995 [28]. As part of a cooperative research and development agreement between the U.S. Department of Energy and University Research Glassware, an improved version of the IOGAPS has been produced and is currently undergoing field testing for PAH and other semi-volatile species. More recently, sorbent-coated denuders have been incorporated into an even higher capacity version, the jumbo-IOGAPS [29]. Two denuders operate as pre-filter strippers for

conventional PS-1 samplers at a total flow of 200 L min^{-1}. A parallel conventional PS-1 has been incorporated into the sampler, and it also collects at 200 L min^{-1}. The jumbo IOGAPS is designed for direct measurement of the phase distributions of trace toxic organic compounds in ambient air.

2. DIRECT DETERMINATION OF SVOC WITH SORBENT-COATED ANNULAR DENUDERS

2.1. Extractable Coatings for Diffusion Denuders

The IOVPS and IOGAPS [14] overcome the main hurdles to direct determination of gas-phase concentrations with denuders: the impossibility of analyzing collected gas-phase compounds directly because of contamination by denuder coating materials or the difficulty of removing the adsorbed species from the coating. An extractable adsorbent coating on the denuder surfaces allows the collected gas-phase material to be removed and quantitated directly; thus, the new diffusion-based samplers are simpler to operate and have fewer potential sources of error than the difference-based diffusion denuder samplers that preceded them. The coating method was discovered by adapting procedures developed for sampling inorganic acid gases with annular denuders, and it is described elsewhere [14]. A slightly modified process [18,22] produces equivalent coatings. The success of this approach depends on the adhesion of the finely ground sorbent particles to sandblasted glass. The coating is resistant to removal by handling, solvent washing and air sampling.

Direct quantitation of species sorbed onto the denuder surfaces has been performed by analysis of solvent extracts. LBNL used cyclohexane for PAH in ETS and ethyl acetate for nicotine in ETS. The denuder coating was intentionally removed after solubilization of the species of interest. The Kamens group and others [17-27] have used solvent mixtures such as hexane, acetone and dichloromethane to extract PAH, nitro-PAH, dioxins and a variety of semi-volatile combustion-generated organics from the XAD-coated surfaces of the IOVPS. They have also shown that coated denuders can be reused at least 20 times before recoating, as long as extraction blanks are monitored regularly [17,18].

2.2. Styrene-Divinyl Benzene Polymer Resins for Air Sampling

XAD-4, a porous macroreticular, non-polar, polystyrene-divinylbenzene resin, was selected as the sorbent for development and validation of the IOVPS and IOGAPS because of its high surface area (725 m^2 g^{-1}) for adsorption of a wide range of SVOC [30]. The chemical structure of polystyrene-divinylbenzene is shown in Figure 1.

The term 'macroreticular' refers to the network of internal channels that results from polymerization in immiscible solvents. These channels enhance the active surface area of the material. Such resins were developed in the 1950's, initially as backbone materials for ion exchange chromatography. Junk, et. al. [31] cautioned that extensive pre-cleaning of the resin beads would be necessary to realize their potential for determination of organics in environmental matrices. In 1966, Hollis [32] described the use of porous polymer beads as the stationary phase for the gas chromatographic separation of a wide range of species. Subsequently, in 1968, Williams and Umstead [33] showed that the porous polymer beads could

be used for sampling halogenated hydrocarbons in air. More recently, XAD-2 and XAD-4 have been used as adsorbents in conventional samplers for the collection of airborne polycyclic aromatic hydrocarbons [34], pesticides [35-37], dioxins [38,39], polychlorinated biphenyls [37,38] and other organic species [40,41].

The IOVPS and IOGAPS use sorbent coatings composed of finely ground XAD-4 particles. Photomicrographs of the coating (Figure 2) show that grinding has broken up the 0.8 mm diameter resin beads into particles with geometric mean diameter of 0.75 μm. Table I shows that grinding enhanced the exposed surface area by about a thousand. London-van der Waals forces hold the coating to the glass surface, enhanced by electrostatic attraction. After preparation, the coating stays on the surface. This is because the adhesive forces on submicron particles are stronger than forces required to dislodge them. Just the opposite is true for larger particles [42]. The coating stability has been verified at LBNL [14] and by Kamens, et al. [17,18] for sampling with the IOVPS up to 30 L min^{-1}.

2.3. Denuder Fluid Dynamics and Efficiency

Gases diffuse orders of magnitude faster than particles at the same temperature. For example, the diffusion coefficients for a particle of 1 μm diameter and a N_2 molecule are $3 \cdot 10^{-7}$ and 0.2 cm^2 sec^{-1}, respectively [42]. Separation by diffusion exploits these properties. Denuders are designed so that while the air stream passes through cylinders or between plates under laminar flow conditions, the gas molecules collide with collecting surfaces that the slower particles never reach. Particles are constrained to move at the linear flow velocity of the air stream. The first diffusion denuders for ambient air sampling were tubes coated with salts [43], and they were used for acidic gases.

The first term of the Gormley-Kennedy equation describes the performance of a cylindrical diffusion denuder when the coating is a perfect sink for the gas molecules. Removal of a gas with diffusion coefficient D is given by

$$\frac{C}{C_0} \approx 0.819 \exp(-14.272\Delta) \qquad (1)$$

where C_o and C are the concentration of the gas at the inlet and outlet of the cylinder and Δ is a first-order decay term,

$$\Delta = \frac{DL}{\gamma R_e d} = \frac{\pi DL}{4F} \qquad (2)$$

that is proportional to the diffusion coefficient D and the active length L of the denuder. Δ is inversely proportional to γ, the air viscosity; $_{Re}$, the Reynolds number; d, the diameter of the tube; and the flow rate F. Equation 1 holds as long as Δ is greater than 0.05. To ensure laminar flow, the Reynolds number should be less than 2000, and an uncoated flow straightening section of the denuder greater than 0.05 d · R_e in length should precede the active collection surface. The efficiency of collection is 1 - C/C_o.

Possanzini, et al. [44] demonstrated that annular denuders had high efficiency at higher flow rates than cylinders with the same inner diameter as the outer diameter of the annulus. A

cross section shows the annulus in Figure 3. Higher flow rates are possible because the annulus is much narrower than the diameter of an equivalent open cylinder. For gas molecules this translates to shorter diffusion path lengths before collision with the walls. When annular denuders have several concentric tubes, higher capacity results from the larger surface area. Because more air can be sampled, limits of detection are lower. Sodium carbonate or bicarbonate-coated annular denuders have been used extensively for sampling nitric and nitrous acids (for example Febo, et al. [45] and references therein).

Possanzini, et al. [44] showed that the removal of gas by a single channel annular denuder with inside and outside diameters d_1 and d_2 can be described by an equation similar to (1) with a decay constant Δ_a

$$\frac{C}{C_0} = 0.82\exp(-22.53\Delta_a) \qquad (3)$$

where Δ_a depends on the annulus dimensions

$$\Delta_a = \frac{\pi DL}{4F}\frac{d_1 + d_2}{d_2 - d_1} \qquad (4)$$

These equations hold when the annulus core diameter d_1 is very much greater than the annulus width d_2-d_1; otherwise the numeric constants must be replaced by terms that depend on the annulus dimensions.

3. THE INTEGRATED ORGANIC VAPOR/PARTICLE SAMPLER (IOVPS)

In 1988, investigators at Lawrence Berkeley National Laboratory recognized the need for accurate measurement of phase distributions of PAH in ETS, and they proceeded to develop an annular denuder with an extractable XAD-4 coating. The idea arose during consideration of the investigators' earlier experience with coating diffusion denuders for sampling nitrous acid. The development of the IOVPS was also influenced by experience gained during attempts at the US EPA in the mid-1980's to make extractable denuder coatings. The first XAD-4 coating onto sandblasted glass was recorded in 1988, and the first IOVPS sampled ETS in late 1991. Researchers at LBNL and the University of North Carolina characterized the performance of the IOVPS between 1992 and 1994. A patent application was filed by LBNL in 1994 [46].

3.1 Design

The first XAD-coated annular denuder was a glass device, 10 cm long, 11 mm in outer diameter, with an 8 mm rod. Small Teflon spacers separated the cylinder and rod. The end caps were Swagelok fittings. The surfaces of the rod and cylinder were sandblasted before they were coated with ground XAD-4. Assembly of the coated pieces was difficult, but operational diffusion denuders resulted. They were used to develop the coating technique and establish that the coating was stable enough for air sampling.

What came to be known as the Integrated Organic Vapor/Particle Sampler was assembled from components manufactured by University Research Glassware in Carrboro, NC, for sampling acid gases. Figure 3 shows a cross section of the IOVPS, including the 1-mm annulus with its coating. Two configurations of the single-channel IOVPS are shown in Figure 4, and each has a size selective inlet to remove particles larger than 2.5 μm from the air stream. They differ in the placement of the 22 cm long denuder sections. To compare collection efficiency to predictions of the Possanzini model (Equation 3), three denuder sections were used in series (Figure 4a), and indoor laboratory room air was sampled at 5-20 L min^{-1} for periods of 3-22 hours [14]. PAH concentrations were determined separately for each section. After validation studies were completed, phase distributions of PAH were measured in environmental tobacco smoke, using the configuration shown in Figure 4b, for up to one hour, at 5-10 L min^{-1}. Two denuder sections were used upstream of the filter pack, and a third denuder downstream collected any PAH that desorbed from the particles during sampling. To increase capacity, multi-channel versions of the IOVPS have been used by other investigators [17-27], in 24 and 40 cm lengths.

The critical difference between the IOVPS and denuders used for sampling gases such as HONO is the coating type, not the hardware design. The IOVPS uses XAD-4 to adsorb a range of gas-phase organic compounds from the airstream, whereas the coating used for HONO is typically sodium carbonate. Acid-base reactions are used to keep the analytes on the denuder surface until extraction and analysis by ion chromatography. In contrast, adsorption of organic species in the IOVPS occurs because of van der Waal's attraction, capillary action and adsorbent-adsorbate pi-electron interactions [47] that are much less powerful than the Coulombic attraction that results in chemical reaction of an acidic molecule with the basic coating. Desorption and migration may also occur during sampling if capacity limits are exceeded. Therefore, trapping equivalent numbers of molecules may require longer and/or larger denuders or longer sampling times and volumes for adsorption-based denuders than for acid-base reaction-based denuders. However, a compensating factor is the fact that the active surface area of the tiny submicron macroreticular resin particles is much greater than the nominal surface area of the denuder. Table II shows the dimensions and predicted performance of a single-channel IOVPS denuder section (with coated length 18.5 cm), from the Possanzini model (Equation 3) for the semi-volatile PAH phenanthrene at 25 °C, with no corrections made for surface sticking coefficients less than 1 or enhanced resin surface area. The diffusion coefficient for phenanthrene is taken from the work of Gustafson and Dickhut [48]. Table II also includes data for two multi-channel versions of the IOVPS that have been used in other studies [17-27].

3.2. Performance Validation

3.2.1. Collection Efficiency

The single-channel IOVPS was evaluated by sampling indoor laboratory air at room temperature (about 21°C). Freshly-coated denuders were used for each test [14]. Two freshly-coated denuders were also used as blanks for each experiment. The room was free of indoor combustion sources. Sampling was performed at 5, 10 and 20 L min^{-1} for 3 and 6 hours, using sampling trains consisting of three single-channel annular denuders and a filter in the configuration shown in Figure 4a. One experiment was done at 20 L min^{-1} for 22 hours. Denuders, filters and sorbent beds (when used) were extracted individually by sonication with high purity cyclohexane. A suite of semi-volatile PAH from naphthalene to chrysene was

analyzed by high performance liquid chromatography with fluorescence detection [14,15,49]. Parallel co-located conventional samplers (filter followed by sorbent bed) were used in some experiments.

For the smaller PAH, the limits of detection were controlled by the amounts found on the XAD-4 coating, and not by the sensitivity of detection. For minimal blanks, potential users should follow the suggestions of Gundel, et al. [14]. Co-located IOVPS yielded PAH concentrations with coefficients of variation that averaged 17%.

Figure 5 shows C/C_o vs denuder length L for the IOVPS for phenanthrene at 5, 10 and 20 L min^{-1} in indoor air and environmental tobacco smoke, compared to predictions of the Possanzini model, Equations 3 and 4. C_o is the sum of the concentrations of phenanthrene collected on each of the three denuder sections. C for one denuder section (L=18.5 cm) is C_o - the sum of the concentrations found on the second and third sections. C for two denuder sections (L=37 cm) is C_o - the concentration found on the third denuder. At 5 and 10 L min^{-1} the third denuder never collected detectable amounts of phenanthrene. The collection efficiency is 1 - C/C_o.

The data are surprisingly close to prediction, even without considering possible multiple adsorption and desorption steps that could occur as semi-volatile molecules pass through the denuder. The good agreement with the Possanzini model indicates that the coated denuder has enough sorbent surface to bring its trapping capacity to near-equivalence with a reaction-based denuder. The data suggest that the IOVPS at 10 L min^{-1} operates at least as well as the Possanzini model predicts for both ETS and ambient air. At 20 L min^{-1} two denuder sections (total coated length of 37 cm) are needed to trap 95% of the phenanthrene from ambient air. The observation of less than predicted collection at 5 L min^{-1} suggests that the transit time (0.16 sec) may be long enough for evaporation from particles [23] to increase the apparent gas phase concentration. Using the decay constants found by Kamens and Coe [23], phenanthrene evaporation from particles during their residence in the single channel IOVPS attenuates the actual phenanthrene particulate concentration by 5, 3 and 1% at the flow rates of 5, 10 and 20 L min^{-1}. However, since only 8% of the total phenanthrene was found in the particle phase [14] in indoor laboratory room air, the extra phenanthrene trapped by the denuder from evaporation of particles would amount to only 5% of the 8% trapped by the filter. This is within the measurement uncertainty, which is also larger at 5 L min^{-1} because the amounts of phenanthrene trapped on the second denuder were close to the limit of quantitation.

Fan, et al. [18] reported collection efficiency data for the four-channel IOVPS (Table II) based on measurements of pyrene that had been vaporized into a 190 m^3 outdoor chamber . They found 92±2% efficiency for collection of pyrene on a single denuder section after 20 min sampling at 20 L min^{-1} whereas Equation 3 predicts 97%. After 20 min sampling at 30 L min^{-1} they found 87±2% efficiency, compared to 90% predicted for pyrene. A possible explanation of the lower collection efficiency for the four-channel denuders [17,18] involves differences in the preparation of the sorbent resin. The coatings used on the multiple-channel denuders were prepared by manual grinding which could not have produced such small particles as those prepared with a planetary ball mill [14,15]. The collection efficiency of the coated multiple-channel denuders would, therefore, be lower due to the smaller surface to volume ratio of the coating particles. Collection efficiency for gas phase pyrene sampled in the 5-channel denuder with 37.5 cm coated length [18] was 100%, and this design was used for most of the published work with multiple-channel denuders [17-27].

3.2.2. Capacity

Another perspective on the performance of the IOVPS is gained by considering that sorbent-based air samplers act like gas chromatography columns. The efficiency of a sorbent-based sampler depends on the concentrations of the sorbed species in the airstream and the amount of sorbent [50]. However, at low concentrations the volumetric capacity depends on the total volume of air sampled and is independent of the gas-phase concentrations of the sorbed species. The holding power of the trap is limited by the amount of air necessary to elute or displace adsorbed material from the surface. At higher inlet gas-phase concentrations the adsorption sites could be filled before the volumetric capacity is exceeded because the weight capacity of the sorbent has been reached.

The gas-phase PAH concentration data obtained from sampling indoor laboratory room air has been used to estimate these limits for the single-channel IOVPS. The goal is bracketing its useful operating range rather than investigating the sorption mechanism in detail. If it is assumed that the volumetric capacity V_g for a particular PAH had been exceeded for total air volumes for which the first denuder collected less than 90% of that PAH, V_g is about 2 m^3 per denuder section for naphthalene (and its methyl derivatives), fluorene and phenanthrene. Four-ring and larger PAH were not detected on second denuders, so V_g could not be determined this way. V_g is somewhat higher for sampling at 10 L min^{-1} for 3 hours, compared to sampling at 5 L min^{-1} for 6 hours. Apparently greater displacement or elution of PAH occurred at the combination of lower flow rate (longer residence time and lower face velocity) and longer total sampling time.

Breakthrough of naphthalene from the second denuder to the third denuder section also occurred when the IOVPS operated at 20 L min^{-1} for 6 and 22 hours. Under those conditions, naphthalene migrated axially along the denuder sections during the extended sampling period, so the volumetric capacity was exceeded. Breakthrough was not observed at 20 L min^{-1} for four-ring or larger PAH. For the other PAH, breakthrough occurred only when sampling at 20 L min^{-1} for 3 hours or longer. The observed breakthrough shows that migration along the denuder sections dominated the collection efficiency for the most volatile species, even though their higher diffusivities compared to the heavier PAH would predict more efficient collection.

The XAD-4 net coating mass was measured by weighing denuders after coating. The weight capacity of ground XAD-4 for naphthalene, fluorene and phenanthrene in indoor air was found to be 57 ± 16, $\geq 4.3 \pm 1.3$ and $\geq 7.7 \pm 3.4$ ng mg^{-1} XAD-4, respectively. The value for naphthalene is about 3 times higher than estimated from breakthrough experiments for an XAD-4 sorbent bed sampler [51]. Therefore a typical IOVPS single-channel denuder section of length 18.5 cm, with nominal glass surface area of 270 cm^2 and 10-15 mg ground XAD-4, can trap about 800 ng naphthalene, 50 ng fluorene and 100 ng phenanthrene.

In summary, the best choice of sampling time and flow rate for the IOVPS depends on the anticipated mass loading in the sampled air, as well as the total amount of air that will pass through the sampler. For sampling source-enriched environmental chambers the limiting factor will probably be the weight capacity of the denuder for the species of interest, but for sampling trace levels in ambient air the volumetric capacity must not be exceeded. For routine use at LBNL [14,15], the second of two single-channel IOVPS (upstream of the filter) was used to assess possible breakthrough.

3.2.3. Particle Transmission Through the IOVPS

Ye, et al. [52] evaluated losses of neutral and charged polydisperse NaCl particles during passage through uncoated annular denuders with the same dimensions as used in this study. At a flow rate of 10 L min^{-1} they found that about 1% of neutral and 6% of singly charged particles with diameters between 0.075 and 1.0 μm and larger were lost per annular denuder section. Losses increased with decreasing particle size, up to about 12% per section for neutral particles of diameter 0.0075 μm. They found less particle loss through denuders that had been coated with sodium chloride or citric acid, compared to uncoated denuders, and they attributed the results to electrostatic effects. In preliminary experiments that used an optical particle counter for ambient particles in fairly dry (30% relative humidity) laboratory room air, we found that, compared to an uncoated denuder, the XAD-4 coating on a single section of the IOVPS reduced particle transmission by about 8% for particle diameters between 0.08 and 2 μm.

However, observed particle losses were always less than 3% during sampling of indoor laboratory room air and environmental tobacco smoke for PAH. Particle losses were assessed by visual examination and estimation of the amount of any observed color change, compared to blanks, for the used XAD-4 coatings after they had been stripped from the denuder surfaces by sonication and collected on Teflon filtration membranes. When ambient air particles were intentionally admitted at loose couplers between denuder sections, the used XAD-4 denuder coatings had a light gray coloration from ambient black (elemental) carbon. Under those conditions the black ambient particles hit the denuder walls because of increased turbulence at the leak site. ETS intentionally admitted between denuder sections caused intensified yellow coloration of the stripped coating. Under normal use the stripped coatings were pale yellowish white. Another symptom of particle loss in those experiments was that concentrations of benz[a]anthracene and chrysene on the affected denuder section were higher than observed on the first (upstream) denuder. This symptom would indicate evaporation of PAH rather than particle loss if there were not parallel evidence for actual particle trapping by the denuder surface (XAD-4 coating color change). Higher molecular weight PAH would also be observed if substantial particle loss occurred.

Fan, et al. [18] evaluated particle loss through the 4-channel IOVPS (Table II) using dioctylphthalate and wood smoke as test aerosols and an optical particle counter. They found high transmission (95-105%) of particles with diameters 0.2-2.5 μm over the flow rate range of 10 - 40 L min^{-1}, but the data showed a slight fall off of penetration as the particle size increased. This was attributed to impaction at the entrance of the denuder. The same research group reported 5-7% particle loss of combustion particles in the longer 5-channel IOVPS (Table II) at 20 L min^{-1} [17-19].

Particle loss was also evaluated for the larger hybrid IOGAPS (discussed in Section 4) by comparing the ambient particulate mass for the IOGAPS filter and the filter in a co-located conventional sampler that operated at the same flow rate. The IOGAPS filter loading was 98% of that measured from the conventional sampler.

3.2.4. Comparison to Filter-Sorbent Bed Sampling

In several studies conventional filter-sorbent bed samplers have been co-located indoors with the single-channel IOVPS and operated for the same time and at the same flow rate. Kamens, et al. [22] and Schauer, et al. [25] have reported that the denuder-based and conventional samplers gave similar total gas and particle concentrations for a range of SVOC with different volatilities and expected partitioning behavior. At LBNL [14] conventional samplers were constructed with a 47-mm diameter filter followed by a sorbent trap that contained between 0.15 and 2.5 g cleaned unground XAD-4 resin beads (20-60 mesh) [53]. Because the two sampler types could yield different phase distributions of all but the most volatile PAH (due to the possibility of sampling artifacts), only species more volatile than phenanthrene (i.e., the naphthalenes, acenaphthene, acenaphthylene and possibly fluorene) would be expected to be trapped with the same efficiency by the sorbents in both sampler types, as long as their capacity limits were not exceeded, i.e., under conditions where there is no breakthrough of gas phase species through the denuder sections.

Gas phase data from sampling indoor laboratory room air on two different days are compared in Table III for two flow rates, 10 and 20 L min-1. Room temperature was 21 oC on each day. Three-hour sampling periods were used for each experiment. Two and three denuder sections were used at 10 and 20 L min-1, respectively (Fig 4b and Fig. 4a respectively). The data indicate that the IOVPS traps and recovers gas phase semi-volatile PAH quantitatively when its capacity is not exceeded. At 10 L min-1 the denuders and sorbent bed trapped the same amounts of semi-volatile PAH. The ratio of detectable PAH measured with the denuders to PAH collected by the sorbent bed was 1.00 + 0.10. Therefore, the IOVPS-derived gas-phase PAH concentrations agreed with the conventional sampler results at this flow rate and sampling time. The data show no apparent sampling artifacts. At the transit time through two sections of the IOVPS (0.16 sec), evaporation of the particulate phenanthrene [23] would have increased the denuder-measured phenanthrene by less than 1% of the actual gas phase concentration. Because the sampling process upsets equilibrium between gas and particulate phases, some temperature dependent desorption of particulate phase PAH is expected [54].

Sampling with the IOVPS for three hours at 20 L min^{-1} yielded gas-phase PAH concentrations (summed from three serial denuder sections) that averaged 79 $\pm$ 11% of those derived from the sorbent bed. The denuder-derived PAH concentrations averaged 73 $\pm$ 9% of the sorbent-derived concentrations for PAH more volatile than phenanthrene (the naphthalenes, acenaphthene, acenaphthylene, biphenyl and fluorene). The capacity limits for these species had been exceeded under the conditions of this experiment.

Denuder-derived concentrations for phenanthrene, anthracene, fluoranthene and pyrene averaged 89 $\pm$ 6% of the sorbent-derived values for the same experiment. Since the data of Figure 5 indicate that phenanthrene was collected in the first two of three denuder sections with > 90% efficiency under the sampling conditions of this experiment, operation of the IOVPS with three serially-connected sections is expected to lead to 99% collection efficiency. In the relatively clean indoor laboratory room air the particulate PAH concentrations were not high enough to increase significantly the apparent gas phase concentrations by evaporation from particles during sampling. However, as discussed below, there is evidence that the apparent sorbent bed concentration of these species increased by "blow off" from the filter-collected particles.

3.2.5. Sampling Artifacts

Table IV shows the phase distribution data for phenanthrene and pyrene collected by the two samplers in indoor laboratory room air at 20 L min^{-1}(Section 3.2.4). Particulate fractions determined from the filter-sorbent bed sampler were smaller than from the IOVPS. The difference was greater for phenanthrene than for pyrene. Since the IOVPS capacity limits were not exceeded, lower gas-phase and higher particulate-phase concentrations measured with the IOVPS for phenanthrene and pyrene are consistent with "blow-off" artifact from the particle-loaded filter in the conventional sampler. Two other parallel sampling experiments also yielded pre-sorbent bed filter samples that had lower PAH concentrations than the filter samples obtained with the IOVPS. Post-filter denuders were not used with the IOVPS in those experiments, so the blow-off-artifact from the IOVPS-collected particles could not be assessed. Such artifacts can be measured directly with the IOVPS when it is configured with a post-filter denuder or sorbent.

Kamens, et al. [17] monitored fluoranthene and pyrene in a chamber filled with diesel exhaust (690 μg m^{-3}). The pyrene concentration was about one hundred-fold higher than in indoor laboratory room air (Table IV). Under these conditions quantifiable amounts of SVOC could adsorb to the collected particles and the filter substrate [55]. They compared a filter-polyurethane foam (PUF) sampler to an IOVPS that had two 4-channel denuders (Table II). When both samplers operated at 20 L min^{-1} at ambient temperature of 24 °C the conventional sampler data showed a positive PAH adsorption artifact of 30-40%, compared to the IOVPS. When the filter-PUF sampler operated at 33 L min^{-1} (at 22 °C) the artifact was negative by 20-30%, i.e., the calculated particulate fraction was lower when data from the conventional sampler were used.

Later work by the same group [18] found negative blow-off artifacts for particulate fluoranthene and pyrene of 15-40% from the conventional sampler, compared to the IOVPS, when the parallel samplers were operated at 30-35 L min^{-1} in chamber air that had a diesel particulate concentration of 260 μm m^{-3} and a temperature near 40 °C. Higher molecular weight compounds (chrysene and benzo[a]pyrene, for example) were not affected. In an experiment at lower chamber temperature (~27 °C) and higher particle loading (600 μm m^{-3}) a positive adsorption artifact was found for particulate fluoranthene and pyrene with the filter-sorbent system when both samplers operated at 15 L min^{-1}. These results suggested that the magnitude and direction of sampling artifacts depended not only on sampler design and flow rate, but also on ambient temperature and the mass concentration of particles.

For assurance of accurate measurement of phase distributions, an optimal sampling system would incorporate a diffusion-based sampler such as the IOVPS for compounds that distribute between the gas and particle phases, such as phenanthrene, fluoranthene and pyrene. The experimental evidence cited above shows that such an approach enables the investigators to minimize sampling artifacts for these compounds. The transit time through the sorbent-coated section should be short enough to limit evaporation of SVOC from the particles (≤0.3 sec from the work of Kamens and Coe [23]). Some parallel measurements should be made with a conventional sampler to assess the possibility of breakthrough of compounds found almost entirely in the gas-phase such as naphthalene. Verification of the transmission of particles through the gas-stripping section is also essential to assure that denuder-collected compounds really originated in the gas phase. Kamens, et al. [23] recommended using both types of

samplers in parallel to acquire the most accurate phase distribution data under a wide range of conditions.

3.3. Phase Distributions of Ambient PAH in Berkeley, CA

A series of six IOVPS were used sequentially over a twenty-four hour period to measure PAH phase distributions at an outdoor site near a roadway at the perimeter of LBNL. Each sampler was configured as indicated in Figure 4b, with a cyclone, denuder and filter followed by another denuder section. Each sampler operated for three and a half hours at 10 L min^{-1}. The particulate fractions of fluoranthene, pyrene, benz[a]anthracene and chrysene are shown in Figure 6 for the six sampling periods that began at 1800 hours on a Sunday evening and continued until the following evening. The temperature ranged from 7 to 18 °C. Amounts of PAH found on the filters and post-filter denuders were attributed to the particulate phase. The particulate fractions varied from 7 to 91% and were higher during the colder periods. It is likely that considerable desorption from collected particles occurred, since roughly two thirds of the particulate PAH fluoranthene, pyrene, benz[a]anthracene and chrysene were found on the post-filter denuders.

Gas/particle partitioning theory [21, 56-58] predicts that, at equilibrium, the semi-volatile PAH will be distributed between the phases according to

$$PAH_g + Particles = PAH_p \qquad (5)$$

where PAH_g and PAH_p represent the gas and particulate phases of a PAH molecule and the term 'Particles' refers to the airborne particulate matter on which the semi-volatile PAH sorb or condense. At equilibrium the constant K describes the partitioning

$$K = \frac{F}{A \bullet P} \qquad (6)$$

where F is the concentration of the particulate PAH (from filters, ng m^{-3}), A is the gas-phase or airborne concentration of the PAH (ng m^{-3}) and P is the mass concentration of particulate matter (μg m^{-3}).

Particulate mass loading for each sampling period was calculated from the 24-hr integrated mass concentration by applying a weighted mass distribution function based on both the elemental black carbon concentrations and the sum of the concentrations of a subset of the particulate semi-volatile PAH for each sampling period. The total mass for the 24-hr period (16.7 μg m^{-3}) was determined from the filter in the hybrid IOGAPS that operated at the same location. Amounts of black carbon for each four-hour period were determined from the measured optical attenuation (blackness) of the particles on each IOVPS filter [59,60]. The mass distribution was calculated from the average of distributions generated from the optical attenuation and the sum of the particulate concentrations of fluoranthene, pyrene, benz[a]anthracene and chrysene were proportional to mass of particles with diameters <2.5 μm. This assumes that the mass of particles smaller than 2.5 μm was proportional to both the particulate PAH and black carbon concentrations.

Figure 7 shows the gas/particle partitioning data for fluoranthene, pyrene and benz[a]anthracene as Arrhenius plots (-log K vs T^{-1}) over the temperature range 7-16°C [29].

The data are consistent with the predictions of Junge-Pankow theory: the higher the ambient temperature, the farther the equilibrium shifts to the left side of Equation 5.

3.4. Phase Distributions of PAH in Environmental Tobacco Smoke

The IOVPS was conceived initially for use in environmental chamber and indoor studies of the phase behavior of PAH and other semi-volatile species in ETS, and it more than met the original expectations. Measured PAH concentrations were typically at least three times higher in ETS than in the relatively clean room air of the laboratory [14]. As Table V shows, PAH could be determined with the IOVPS in as little as 1 hr of sampling at 5 L min^{-1} after three reference cigarettes were machine-smoked in a sealed 36 m^3 chamber at 16°C. Emission factors based on these data are given in Gundel, et al. [15], along with details of the sampling and analytical methods.

None of the more volatile PAH from naphthalene to anthracene were detected on the ETS particles, but fluoranthene and pyrene were found in both phases. Very little benz[a]anthracene and chrysene were found in the gas phase ETS. Generally, the particulate fraction increased as molecular weight increased and vapor pressure decreased [61,62]. No detectable amounts of PAH were found on the second filters or the post-filter denuders. No "blow-off" of particulate PAH onto the backup filter substrate or downstream denuder was observed for this experiment. In a separate experiment using the same IOVPS configuration but with the chamber at 20 °C, fluoranthene, pyrene and chrysene were detected on the post-filter denuder, not on the backup filter, indicating that some blow-off occurred. The amounts found on the post-filter denuder averaged 16% of the total particulate PAH concentrations. The single-section capacity limits were not exceeded, since no PAH were detected on the second (pre-filter) denuder in the experiment at 20 °C.

The particulate fractions were much higher for ETS than for indoor air with no combustion sources (Table IV). Since the face velocities were different, interpretation of differences in phase distributions for the two environments must be made cautiously. However, lower fractions of particulate-phase PAH in ambient air are consistent with the presence of "dried out" aged particles, compared to oily ETS particles that were freshly emitted. "Blow-off" of semi-volatile PAH from the indoor particles would be expected to occur to a larger extent at the higher face velocity and longer sampling time used in the indoor sampling. However, the phase distributions obtained for PAH in indoor air with the two sampler types do not overlap the range observed for the same PAH in ETS. Several of the ambient (outdoor) PAH measured six times over a 24-hr period at 10 L min^{-1} had average particulate fractions between those observed in indoor air and ETS: fluoranthene, 0.22±0.23; benz[a]anthracene, 0.47±0.17; chrysene, 0.61±0.22. The higher particulate PAH fractions observed in ETS are consistent with gas/particle partitioning theory [56-58]. Figure 8 shows ETS chamber data from five experiments obtained with the IOVPS for phenanthrene, pyrene and benz[a]anthracene] as Arrhenius plots (-log K vs T^{-1}) over the temperature range 16-25°C [63]. In these experiments the IOVPS sampled at 5-10 L min^{-1} for 20-40 min, starting about 10 min after the end of machine smoking. The mass loading of respirable suspended particulate matter (RSP, <2.5 μm diameter) in was roughly 1 mg m^{-3}. Benz[a]anthracene data for ETS and ambient air apparently followed the same partitioning equilibrium. This was not true for pyrene for which the partitioning constants differed significantly.

3.5 Phase Distributions of Nicotine in Environmental Tobacco Smoke

The IOVPS has been used very successfully to investigate gas/particle partitioning of nicotine (a semi-volatile alkaloid) in ETS as part of studies of its dynamic behavior and fate [64,65]. Figure 9 shows the gas and particulate concentrations of nicotine over a three hour period at 24 °C during and after the burning of three cigarettes by machine in a sealed 20 m^3 chamber with stainless steel walls. Sampling used five IOVPS that operated sequentially at 5 L min^{-1} for three ten-minute periods, followed by two twenty-min periods during the second half of the experiment. The data shown in Figure 9 and data from similar experiments at LBNL clearly demonstrated that gas phase nicotine decayed more quickly than nicotine in the particulate phase, and that condensation onto ETS particles was not a dominant decay mechanism. Figure 10 shows the concentration of gas phase nicotine as a function of time after smoking for the same experiment as determined from the IOVPS and small co-located XAD-4 sorbent tubes. Just after the fifth IOVPS sample was collected the chamber was vented for two hours, then resealed for three hours. During the last hour a final sorbent sample was collected to assess re-emission of nicotine from the walls. Wall deposition proved to be the ultimate fate of more than 90% of the gas phase nicotine, and the data from this and experiments with pure nicotine were incorporated into a non-linear reversible sorption model [64,65].

3.6 The IOVPS in Other Applications

Although direct determination of the gas phase of SVOC with the IOVPS has been possible only relatively recently, several research groups in the United States have already used the new sampling technology to investigate significant issues in gas/particle partitioning. Highlights of some of these efforts are summarized below.

3.6.1 Kinetics of the Formation and Decay of Nitro-PAH

With assistance from its inventors at LBNL and the US EPA, researchers at the University of North Carolina have used multi-channel versions of the IOVPS since early 1992, after they learned that LBNL was developing an XAD-coated denuder for SVOC. Fan, et al. incorporated the IOVPS for sampling semi-volatile PAH and nitro-PAH as part of the Kamens group's ongoing atmospheric chemistry research program [17-24, 26]. They have made important contributions to validation of the IOVPS, as mentioned above, and they have used it extensively to enhance understanding of gas/particle partitioning and the atmospheric chemistry of PAH, nitro-PAH and dioxins.

They chose to use the IOVPS to study the kinetics of the formation and decay of nitro-PAH in irradiated diesel exhaust because they needed to measure accurately both the gas and particulate concentrations of semi-volatile reactants and products. Their earlier work had suggested that sampling artifacts compromised the results based on filter-sorbent sampling [17]. Using the IOVPS they found the nitro-PAH photochemical products of pyrene and fluoranthene entirely in the particulate phase [17,18], in contrast to earlier work that suggested the products were distributed between the phases. They concluded that formation of nitro-PAH in the gas phase from OH and NO_2 reactions was followed by very rapid association of nitro-PAH with the diesel particles. Later work with the IOVPS in smog chamber studies of diesel and wood smoke showed that the particulate phase nitro-PAH decayed quickly in sunlight [19] and that degradation by ozone could only be important at night [20]. The IOVPS-generated data were

incorporated into an updated photochemical mechanism for the formation and decay of nitro-PAH [20,24].

3.6.2 Atmospheric Behavior of Dioxins

Penisse and Kamens [26] used a five-channel version of the IOVPS in studies of the atmospheric behavior of polychlorinated dibenzo-p-dioxins and dibenzofurans. The dioxins and furans were generated in an environmental chamber by burning wood chips that had been treated with an environ chamber pentachlorophenol or plastic pipe shavings made from polyvinyl chloride. They found that only the tetra and pentachlorinated dioxins and furans partitioned into the gas phase under the high particle loadings they used. Total suspended particulate matter concentrations ranged from 1 to 7 mg m^{-3}. The particulate phase polychlorinated species that had been generated during high temperature combustion were more stable to photodegradation than those generated during low temperature combustion.

3.6.3 Kinetics and Thermodynamics of Gas/Particle Partitioning

The IOVPS has been used in several recent studies of the dynamics of gas/particle partitioning. To investigate the time necessary to achieve equilibrium, Kamens, et al. [22] monitored the rates of migration of semi-volatile PAH to diesel particles at 22-25 °C in a large smog chamber. The IOVPS was used to measure the gas and particulate phase concentrations from which apparent equilibrium constants were calculated. The system did not depart much from equilibrium at this temperature and thus equilibrium partitioning theory applied. However, at -1 to -4 °C wood smoke particles could not outgas fast enough to restore equilibrium as gas PAH were lost to the chamber walls.

In a related study, Odum, et al. [21] monitored the time evolution of the phase distribution of deuterated pyrene after diesel particles were admitted to a smog chamber that initially contained gas-phase d_{10}-pyrene. From the data they derived a plausible diffusion constant and surface mass transfer coefficient for deuterated pyrene into diesel particles that were assumed to have a liquid organic layer surrounding a solid carbon core. They concluded that mass transfer and thus time to equilibrium are dependent on ambient temperature and humidity as well as particle size and the vapor pressure of the partitioning compound.

Recently Kamens and Coe [23] applied and refined these insights when they measured particle outgassing in a large carbon-filter parallel plate multi-channel denuder that was filled with diesel exhaust at high concentrations. Transit time was varied over the range of 2 to 11 sec by adjusting the flow rate. They used IOVPS units upstream and downstream of the stripper to observe changes in the phase distribution as the exhaust passed through the large denuder. They were able to estimate first order rate constants for evaporation of particulate phenanthrene and fluorene at two temperatures. Their results suggest that, at least for sampling high particulate concentrations at warm ambient temperatures, residence times through the IOVPS should be kept as short as consistent with controlling breakthrough. They calculated that about 10% of the particulate phenanthrene and fluorene evaporated as they passed through the IOVPS with residence time of 0.3 sec at around 20 °C.

3.6.4 Semi-Volatile Organic Compounds from Combustion Sources

On-going combustion source emission characterization efforts at the California Institute of Technology (Cal Tech) include sampling and analysis of semi-volatile organic species from a

variety of in-use vehicles [25]. These studies incorporate parallel sampling trains downstream of a dilution chamber: a 40 cm, 4-channel IOVPS with PUF backup and a conventional filter-PUF sampler. Each side operates at 30 L min^{-1}. A wide range of gas and particulate organic species are quantified by gas chromatography with flame ionization and mass spectrometric detection and other techniques. Schauer, et al. [25] have shown that the IOVPS and conventional samplers agree in total mass for all compounds, but the phase distributions differ for semi-volatile species. The results show that the IOVPS can be used for quantification of many individual species in the complex mixture of organics found in vehicle exhaust.

3.6.5 Semi-Volatile Organic Compounds in Secondary Aerosols

Photochemical reactions involving reactive organic gases lead to the formation of ambient secondary organic aerosol, and major uncertainty exists regarding the phase behavior of semi-volatile oxidation products [66]. Recently Odum, et al. [67] at Cal Tech applied Pankow's model of absorption of SVOC into organic layers on particles to smog chamber studies. They developed a gas/particle partitioning model that related the aerosol yields from reactive gases to the amount of organic mass available. The first experimental verification of the model depended on monitoring gas concentrations and aerosol characteristics in an outdoor smog chamber. They concluded that due to partitioning of SVOC, unique aerosol yields could not be determined for individual compounds because the amounts formed depended on the total aerosol mass concentration. Subsequent work by Odum, et al. [27] with a 40-cm, 5-channel IOVPS includes measurements of the phase distributions of actual photochemical reaction products from individual hydrocarbons. The results support the partitioning theory and suggest that smog chamber measurements of hydrocarbon mixtures can be used to model atmospheric secondary organic aerosol formation.

4. THE INTEGRATED ORGANIC GAS AND PARTICLE SAMPLER (IOGAPS)

Diffusion-based sampling for SVOC in the ambient atmosphere requires higher capacity for semi-volatile organics than the various IOVPS designs can provide. To meet the need for collection over 12-48 hr periods at flow rates up to 200 L min^{-1}, we have developed a series of higher capacity denuder-based samplers. The new design is called the Integrated Gas and Particle Sampler because the first prototype used the IOVPS coating on a modified Gas and Particle (GAP) sampler. The IOGAPS has been developed through a collaboration between LBNL and Environment Canada. Table VI lists the design characteristics and predicted trapping abilities for the three types of IOGAPS that had been constructed by the end of 1996. The hybrid IOGAPS was used to sample ambient particulate matter in Berkeley, CA (28]. The IOGAPS, a more portable version with smaller annuli than the hybrid IOGAPS, is indicated in Table VI as the IOGAPS. The jumbo-IOGAPS is a prototype high capacity sampler that incorporates two parallel denuders into two PS1 filter-sorbent units. Compared to the IOVPS, the denuders in these samplers have roughly twice the outer diameter and three times the active length of the single-channel IOVPS used at LBNL [14,15]. Their coated area is about thirty times more than a single-channel IOVPS [14,15] and about four times the area of the long multi-channel IOVPS [17-27].

4.1. The Prototype IOVPS-GAP Hybrid Sampler

The major difference between the GAP sampler [8] and the hybrid IOGAPS is the type of coating. A schematic diagram of the hybrid IOGAPS is shown in Figure 11. A single GAP unit has two sampling trains, one with and one without a coated multi-channel denuder. Filters and downstream sorbent beds are included with each train. Each side has a size selective inlet to remove particles greater than 10 μm in aerodynamic diameter at 16.7 L min^{-1}. The original GAP annular denuder used crushed Tenax resin on silicone gum (gas chromatographic column support material) as the adsorbent for semi-volatile organochlorine pesticides [9] and PAH [68]. As mentioned above, the GAP sampler provided gas phase concentrations as the difference between the amounts found from the conventional and the denuder sampling trains. In contrast, the hybrid IOGAPS has ground XAD-4 on the denuder surfaces. Before coating, the glass tubes had been sandblasted at LBNL to make tracks of average width 50 μm, as observed with optical microscopy. Coating, extraction and analytical procedures developed for the IOVPS [14] were adapted for the larger hybrid IOGAPS as described in Reference 28. Teflon-coated glass fiber filters and XAD-4 unground resin were used for particles and back up adsorbers, respectively. When the hybrid IOGAPS was used to sample ambient PAH at LBNL, a second identical hybrid IOGAPS on site provided field blank data.

4.1.1. Polycyclic Aromatic Hydrocarbons in Berkeley, CA

In April 1995, preliminary field testing was carried out with the hybrid IOGAPS at an outdoor location at LBNL over a 24-hr period. Because all components of the GAP sampler, including the denuder, could be quantitatively extracted for the PAH collected, we had the opportunity to compare the efficiency of the high-capacity XAD-4 coated denuder with the built in parallel conventional sampling system. The denuder of the IOGAPS retained the gas phase PAH whereas the filter and two downstream adsorbers yielded the particle phase, unless there was breakthrough from the denuder. For the conventional sampling train (without denuder) the total PAH were determined by adding amounts found on the filter and the adsorbers. Both sampling trains operated at 16.7 L min^{-1} (1 m^3 hr^{-1}). Apparent gas and particulate PAH concentrations were found from amounts on the filter and the sum of amounts found in the downstream adsorbers, respectively. The filter-derived mass concentrations agreed to within 2% for both sampling trains, indicating that particle loss through the denuder was insignificant.

Table VII shows the blank-corrected PAH results for both sides of the hybrid IOGAPS and the IOVPS. Data from parallel sampling with six sequential IOVPS are included as 24-hr averages, except for the naphthalenes, where data are only available for the first 20 hr. The PAH are grouped in order of increasing aromatic ring size and decreasing volatility. In general, the three sampler types agreed reasonably well for total PAH.

Quantitation of the naphthalenes was complicated by fluorescence detector overload for the 24-hr integrated samples. After recognition of the detector overload condition for naphthalenes from the 24-hr integrated hybrid IOGAPS and conventional samplers, the instrument was recalibrated using higher concentration standards, and the response was corrected for the observed self-absorption by analyzing diluted aliquots. We estimate that this process increased the uncertainty in quantitation from an average of 15% for all PAH to 60% for the naphthalenes. Therefore the IOGAPS and conventional samplers agree in amounts of the total naphthalenes within this experimental uncertainty. Nevertheless, the data show that some breakthrough occurred for the naphthalenes from the hybrid IOGAPS, because the first post-filter

sorbent had about 10% of the total naphthalene, but less than 1% of the naphthalene was found on the post-filter denuder in the IOVPS. We expect that the narrower annuli of the newer IOGAPS will overcome this limitation. Table VI shows predicted enhancements of more than two orders of magnitude in trapping ability of with the new design.

The limited data available for phenanthrene indicate that this PAH was found primarily in the gas phase for both sampler types, with the IOGAPS collecting a higher particulate fraction. For anthracene, fluoranthene and pyrene the apparent partitioning between gas and particle phases was dependent on the sampler type. Data from both the IOVPS and the hybrid IOGAPS data suggest significantly higher particulate fractions than data from the conventional sampler. This is consistent with evaporation from collected particles "blow-off" artifacts for the conventional sampler that would lead to overestimation of the gas phase concentration. The limited data for benz[a]anthracene and chrysene suggest equal partitioning between the gas and particulate phases with no pronounced sampler-related differences.

For PAH of 5 or more rings, the entire mass of each compound was found on the filter. For these compounds, the agreement between the hybrid IOGAPS and the conventional sampler was better than 80%, which is within the expected experimental uncertainty [15].

4.1.2. Comparison to IOVPS

The IOVPS-derived concentrations of the naphthalenes were lower than the other samplers, and this was likely due to the loss of IOVPS data for the last sampling period (2-6 p.m. on a workday). The IOVPS naphthalene 20-hr averages were probably lower than the 24-hr average would have been because data for the other PAH and the time profiles for all PAH indicated that local traffic contributed to higher than average emissions during the evening commute from LBNL during the sixth sampling period. There was no evidence for significant breakthrough of naphthalene through the two denuder sections of the IOVPS for the conditions of this field test.

Generally data from the IOVPS and hybrid IOGAPS showed the same gas/particle partitioning behavior. If particles had evaporated during the 2.6 sec transit through the hybrid IOGAPS [23], the particulate fractions would have been lower for the IOGAPS than for the IOVPS, but the available data show little evidence for this.

4.3. Design Parameters for the IOGAPS

As part of a cooperative research and development agreement between the US Department of Energy and University Research Glassware, Inc. a more compact and rugged version of the high capacity IOGAPS has been developed. The IOGAPS incorporates a size selective (cyclone) inlet for particles less than 2.5 μm, a newly designed denuder, a 47-mm filter and downstream adsorber, as well as a parallel conventional sampler with a similar cyclone. Table VI shows that because the denuder annuli are narrower, its predicted stripping power is about three orders of magnitude higher than for the hybrid IOGAPS at the same flow rate. With appropriate size selective inlets the IOGAPS is intended to sample at up to 75 L min^{-1}. The housing has been designed to operate at temperatures as low as -40C where, because of the relationship of diffusion coefficient and temperature, the collection efficiency of the denuders and hence C/Co will be poorest. Even under those conditions, naphthalene should have a C/Co of better than 98%. The IOGAPS is currently the subject of validation and field studies being conducted by the authors.

4.4. Jumbo-IOGAPS

Recognition of the need for accurate measurements of gas/particle partitioning of trace organic species such as dioxins [69] led to the development of an even higher capacity diffusion-based sampler that can used with PS-1 units. The new prototype dual-annular denuder sampler has been dubbed the Jumbo-IOGAPS because of its size and its intended total flow of 200 L min^{-1} (100 L min^{-1} per channel). The Jumbo (Figure 12) also has a built-in conventional PS-1 sampler (200 L min^{-1}). The exposed filter collection areas of the denuder and conventional sampling trains have been modified so that the face velocities are equal. The new very high capacity sampler is currently undergoing validation and field studies at LBNL, and it shows promise for collection of sufficient material for phase distribution studies of a wide range of trace organic species in the ambient atmosphere.

5. SUMMARY AND CONCLUSIONS

Sorbent-coated annular denuder-based samplers have been developed for direct determination of both gaseous and particulate semi-volatile organic species. The first such sampler, the Integrated Organic Vapor/Particle Sampler, has been validated for sampling semi-volatile PAH in ambient air and environmental tobacco smoke. Multi-channel versions of the IOVPS have been used successfully for investigation of gas/particle partitioning of a variety of semi-volatile organic species in combustion source-enriched environmental chambers. Subsequent improvements have resulted in two new higher-capacity samplers, the IOGAPS and the jumbo-IOGAPS, that use the same sorbent for sampling trace organics in the ambient atmosphere for 24-48 hr periods over a wide temperature range. Construction of these new samplers began by incorporating the IOVPS coating technology onto the gas collection surfaces of the higher capacity GAP sampler. Substantial design effort aims to ensure that vapor phase components as volatile as naphthalene can be trapped efficiently and retained by the sorbent-coated surface while the particles pass through to the filter.

The chief significance of the development of sorbent-coated diffusion denuders is that phase distributions of a wide range of semi-volatile organic species can now be made directly, rather than by difference or by techniques that are subject to large positive and negative artifacts. The IOVPS and IOGAPS fill long-recognized needs for diffusion-based sampling methods for airborne semi-volatile organic compounds.

6. ACKNOWLEDGMENTS

The authors thank Joan M. Daisey and Robert K. Stevens, for inspiration and encouragement; Victor C. Lee for patient and thorough development of the XAD coating process; Hector G. Cancel-Velez for assistance with field testing of the IOVPS; Kariyawasam R.R. Mahanama for developing the PAH detection method for ETS; Richard Lamens, Zhi-Hua Fan, Jay R. Odum, James J. Schauer and Glenn Cass for keeping us informed about research progress with various versions of the IOVPS.

7. REFERENCES

1. T. Colburn, F.S. vom Saal, and A.M. Soto, *Environ. Health Perspec.* **101** (1993): 378- 384.
2. T.F. Bidleman, *Environ. Sci. Technol.* **22** (1988): 361-367.
3. J.T. Hoff, R. Gillham, D. Mackay and W.Y. Shiu, *Environ. Sci. Technol.* **27** (1993): 2174-2180.
4. S. Paterson, D. Mackay and C. Mcfarlane, *Environ. Sci. & Technol.* **28** (1994): 2259-2266.
5. National Research Council, Committee on Passive Smoking, ed., Exposure-dose relationships for environmental tobacco smoke, in *Environmental Tobacco Smoke: Measuring Exposures and Assessing Health Effects* (1986): National Academy Press, Washington, DC, pp. 120-132.
6. R.C. Flagan, and J. Seinfeld, *Fundamentals of Air Pollution Engineering*. (1988): Prentice-Hall, Englewood Cliffs, NJ.
7. C.E. Cowan, D. Makay, T.C.J. Feijtel, D. van de Meent, A. Di Guardo, J. Davies, N. Mackay, The Multi-Media Fate Model: A Vital Tool for Predicting the Fate of Chemicals, (1995): SETAC Press, Penascola
8. D.A. Lane, N.D. Johnson, S.C. Barton, H.S. Thomas and W.H. Schroeder, *Environ. Sci. Technol.* **22** (1988): 941-947.
9. D.A. Lane, N.D. Johnson, M.-J.J. Hanley, W.H. Schroeder and D.T. Ord, *Environ. Sci. Technol.* **26**, (1992): 126-133
10. R.W. Coutant, L. Brown, J.C. Chuang, R, Riggan and R.G. Lewis, Atmos. Environ. 22 (1988): 403-409.
11. R.W. Coutant, P.J. Callahan, J.C. Chuang and R.G. Lewis, *Atmos. Environ.* **26A** (1992): 2831-2834.
12. D.J. Eatough, B. Sedar, L. Lewis, J.D. Hansen, E.A. Lewis and R.J. Farber, *Aerosol Sci. Technol.* **10** (1989): 438-449.
13. D.J. Eatough, A. Wadsworth, D.A. Eatough, J.W. Crawford, L.D. Hansen and E.A. Lewis, *Atmos. Environ.* **27A** (1993): 1213-1219.
14. L.A. Gundel, V.C. Lee, K.R.R. Mahanama, R.K. Stevens and J.M. Daisey, *Atmos. Environ.* **29** (1995): 1719-1733.
15. L.A. Gundel, K.R.R. Mahanama and J.M. Daisey, *Environ. Sci. Technol.* **29** (1995): 1607-1614.
16. T.L. Vossler, R.K. Stevens, R.J. Paur, R.E. Baumgardner and J.P. Bell, *Atmos. Environ.* **22** (1988): 1729-1736.
17. R.M. Kamens, Z.H. Fan, Y. Yao, D. Chen, S. Chen and M. Vartianen, *Chemosphere*, **28** (1994): 1623-1632.
18. Z. Fan, D. Chen, P. Birla and R.M. Kamens, *Atmos. Environ.* **29** (1995): 1171-1181.
19 Z.H. Fan, R.M. Kamens, J.X. Hu, J.B. Zhang and S. McDow, *Environ. Sci. Technol.* **30** (1996): 1358-1364.
20. Z. Fan, R.M. Kamens, J. Zhang and J. Hu, *Environ. Sci. Technol.* **30** (1996): 2821-2827.
21. J.R. Odum, J.Z. Yu and R.M. Kamens, *Environ. Sci. Technol.* **28** (1994): 2278-2285.
22. R. Kamens, J. Odum and Z. Fan, *Environ. Sci. Technol.* **29** (1995): 43-50.
23. R.M. Kamens and D.L. Coe, *Environ. Sci. Technol.* **31** (1997): 1830-1833.
24. R.M. Kamens, Z. Fan, M. Jang, J. Odum, J. Hu, D. Coe, J. Zhang, S. Chen and K. Leach, Gas and particle partition measurements of atmospheric organic compounds, D.A. Lane, ed. in

Advances in Environmental Process Control Technologies, (1997, in press): Gordon and Breach, Newark.

25. J.J. Schauer, M. Kleeman, G.R. Cass and B.R. Simoneit, Development of a comprehensive dilution source sampler for collection of size-segregated aerosol, semivolatile organic compounds and volatile organic compounds suitable for trace level quantification, presented at the annual meeting of the American Association for Aerosol Research, October 14-18, 1996, Orlando, Fl.
26. D.M. Pennise and R.M. Kamens, *Environ. Sci. Technol.* **30** (1996): 2832-2842.
27. J. Odum and J. Seinfeld, Gas-particle partitioning and yields of secondary organic species, presented at the symposium on semi-volatile organics, American Chemical Society, 211th Annual Meeting, March 24-28, 1996, New Orleans, LA.
28. D.A. Lane and L.A. Gundel, *Polycyclic Aromatic Compounds* **9** (1996): 67-73.
29. D.A. Lane and L.A. Gundel, The Integrated Gas and Particle Sampler for Semi-Volatile and Particulate Organic Pollutants. Presented at the American Association for Aerosol Research meeting, October 14-18, 1996, Orlando, FL.
30. Rohm and Haas Co. (1993) Amberlite XAD-4 Polymeric Adsorbent. Technical Bulletin 1E403, Rohm and Haas Co., Spring House, PA 19477.
31. G.A. Junk, J.J. Richard, M.D. Grieser, D. Witiak, J.L. Witiak, M.D. Arguello, R. Vick, H.J. Svec, J.S. Fritz and G.V. Calder, *J. Chromatog.* **99** (1974): 745-762.
32. O.L. Hollis, *Anal. Chem.* **38** (1966) 309-316.
33. F.W. Williams and M.E. Umstead, *Anal. Chem.* **40** (1968): 2232-2234.
34. F.J. Offermann, S.A. Loiselle, A.T. Hodgson, L.A. Gundel and J.M. Daisey, *Indoor Air* **1**, (1991): 497-512.
35. J.N. Seiber, D.E. Glotfelty, A.D. Lucas, M.M. McChesney, J.C. Sagebiel and T.A. Wehner, *Arch. Environ. Contam. Toxicol.* **19** (1990): 583-592.
36. C.J. Schomburg, D.E. Glotfelty and J.N. Seiber, *Environ. Sci. Technol.* **25** (1991): 155-160.
37. H. Kaupp and G. Umlauf, *Atmos. Environ.* **26A** (1992): 2259-2267.
38. D.J. Wagel, T.O. Tierman, M.L. Taylor, J.H. Garrett, G.F. Van Ness, J.G. Solch and L.A. Harden, *Chemosphere* **18** (1989): 177-184.
39. G. Lebel, D.T. Williams, B.R. Hollebone, C. Shewchuk, L.J. Brownlee, H. Tosine, R. Clement, and S. Suter, *Intern. J. Environ. Anal. Chem.* **38** (1990): 21-29.
40. K.E. Noll and J.N. Sarlis, *J. Air Poll. Control Assoc.* **38** (1988): 1512-1517.
41. J.O. Levin, K. Andersson and R.M. Karlsson, *J. Chromatog.* **454** (1988): 121-128.
42. W.C. Hinds, Aerosol Technology: Properties, Behavior and Measurement, 1982 Wiley-Interscience, New York, 424 pp.
43. R.K. Stevens, T.G. Dzubay, G.M Russwurm and D. Rickel, *Atmos. Environ.* **12** (1978): 55-68.
44. M. Possanzini, A. Febo and A. Liberti, *Atmos. Environ.* **17** (1983): 2605-2610.
45. A. Febo, C. Perrino and M. Cortiello, *Atmos. Environ.* **27A** (1993):1721-1728.
46. L.A. Gundel, J.M. Daisey and R.K. Stevens, Quantitative Organic Vapor-Particle Samplers, U.S. Patent 8,431,358, 1995.
47. A.V. Kiselev and Y.I. Yashin, *Gas-Adsorption Chromatography.* 1969 Plenum, New York, p.11-16.
48. K.E. Gustafson and R.M. *J. Chem. Eng. Data* **39** (1994): 286-289.

49. K.R.R. Mahanama, L.A. Gundel and J.M. Daisey, *Intern. J. Environ. Anal. Chem.* **56** (1994): 289-309.
50. J. Adams, K. Menzies and P. Levins, Selection and evaluation of sorbent resins for organic compounds. (1977) U.S. Environmental Protection Agency Report EPA 600/7-77-044.
51. F.J. Offermann, S.A. Loiselle, J.M. Daisey, A.T. Hodgson and L.A. Gundel, Sampling, analysis and data validation of indoor concentrations of polycyclic aromatic hydrocarbons, final report to the California Air Resources Board, (1990) Contract No. A732-106.
52. Y. Ye, C.-J. Tsai, D.Y.H. Pui and C.W Lewis, *Aerosol Sci. Technol.* **14** (1991): 102-111.
53. S.A. Loiselle, A.T. Hodgson and F.J. Offermann, *Indoor Air* **2** (1991): 191-210.
54. X. Zhang and P.H. McMurry, *Environ. Sci. Technol.* **25** (1991): 456-459.
55. S.R. Mc Dow and J.J. Huntzicker, *Atmos. Environ.* **24A** (1990): 2563-2571.
56. J.F. Pankow, *Atmos. Environ.* **21** (1987): 2275-2283.
57. J.F. Pankow, *Atmos. Environ.* **26A** (1992): 2489-2497.
58. J.F. Pankow, L.M. Isabelle, D.A. Buchholz, W. Luo and B.D. Reeves, *Environ. Sci. Technol.* **28** (1994): 363-365.
59. L.A. Gundel, R.L. Dod, H. Rosen and T. Novakov, *Sci. Total Environ.* **36** (1983): 197-202.
60. H. Rosen, A.D.A. Hansen, L. Gundel and T. Novakov, *Appl. Opt.* **17** (1978): 3859-3861.
61. C. Pupp, R.C. Lao, J.J. Murray and R.F. Pottie, *Atmos. Environ.* **8** (1974): 915-925.
62. W.J. Sonnefeld, W.H. Zoller and W.E. May, *Anal. Chem.* **55** (1983): 275-280.
63. L.A. Gundel, M.D. Van Loy and J.M. Daisey, Gas/Particle Partitioning of Polycyclic Aromatic Hydrocarbons in Environmental Tobacco Smoke. Presented at the American Association for Aerosol Research Annual Meeting 1996, October 14-18, Orlando, FL.
64. M.D. Van Loy, W.W. Nazaroff, V.C. Lee, L.A. Gundel, R.G. Sextro and J.M. Daisey, Investigation of the fate of nicotine in a stainless-steel chamber. Presented at the 89th Annual Meeting and Exhibition of the Air and Waste Management Association, June 23-28, 1996, Nashville, TN.
65. M.D. Van Loy, V.C. Lee, L.A. Gundel, J.M. Daisey, R.G. Sextro and W. W Nazaroff, *Environ. Sci. Technol.* **31** (1997): 2554-2561.
66. S.N. Pandis, R.A. Harley, G.R. Cass, J.H. Seinfeld, *Atmos. Environ.* **26A** (1992): 2269-2282.
67. J.R. Odum, T. Hoffmann, F. Bowman, D. Collins, R.C. Flagan and J.H. Seinfeld, *Environ. Sci. Technol.* **30** (1996): 2580-2585.
68. D.A. Lane and N.D Johnson. *Polycyclic Aromatic Hydrocarbons* **13, Supplement**, (1993): 511-518.
69. L.A. Gundel, Measurement of phase distributions with diffusion denuders, presented at the EPA Dioxin Workshop on Deposition and Reservoir Sources, Washington, DC, July 22-24, 1996.

8. TABLES

Table I. Comparison of surface characteristics of ground and unground XAD-4 resin.

Table II. Design parameters for single- and multi-channel versions of the Integrated Organic Vapor/Particle Sampler. The predicted fraction of outlet to inlet gas phase concentrations for one denuder section, C/C_o, is illustrated for phenanthrene at 25°C.

Table III. Comparison of the IOVPS to a filter-sorbent bed sampler for collection of gas-phase PAH in indoor air at two flow rates.

Table IV. Phase distributions of phenanthrene and pyrene in indoor laboratory room air at 21 °C for co-located IOVPS and filter-sorbent bed samplers at 20 L min^{-1} for 3 hr.

Table V. Phase distributions of polycyclic aromatic hydrocarbons in simulated environmental tobacco smoke at 16 °C.

Table VI. Design parameters for high capacity Integrated Organic Gas and Particle Samplers. The predicted fraction of outlet to inlet gas phase concentrations for one denuder section, C/C_o, is illustrated for phenanthrene at 25°C.

Table VII. Comparison of PAH concentrations for a 24-hr period April, 1995, in Berkeley, CA, as measured by three sampler types: The hybrid IOGAPS, a conventional filter-sorbent sampler and six sequentially operated IOVPS.

9. FIGURES

Figure 1. The chemical structure of styrene-divinylbenzene copolymer macroreticular resins such as XAD-2, XAD-4, XAD-16, Chromosorb 102 and Ostion SP-1. Adapted from US Patent 4,224,415, R.M. Patel, et al., American Laboratory, Feb. 1990, and G.A. Junk, Symposium on Solid Phase Extraction, American Chemical Society, 205th Annual Meeting, San Francisco, Mar. 28-Apr. 2, 1992.

Figure 2. Scanning electron photomicrographs of (top) an uncoated sandblasted glass annular denuder fragment, and (bottom) an annular denuder fragment coated with ground XAD-4 adsorbent. The instrument was operated at 20 keV, 50 μm beam, 26° tilt and 12-mm working distance.

Figure 3. Cross section of a single channel coated annular denuder. The dimensions shown apply to the Integrated Organic Vapor/Particle Sampler (IOVPS).

Figure 4. Sampling configurations for the IOVPS. The arrows show the direction of airflow. d1, d2 and d3 indicate XAD-4-coated glass annular denuder sections, each with coated length of 18.5 cm, that are connected by threaded couplers. Cross-sectional dimensions are shown in Figure 3.

The filter pack holds one or two 47-mm diameter filters. (a) The configuration used for initial testing and validation studies in combustion-free indoor air. (b) The configuration used for sampling simulated environmental tobacco smoke in an environmental chamber. This configuration was also used for phase distribution measurements in outdoor ambient air.

Figure 5. The ratio of outlet concentration of phenanthrene C to inlet concentration C_o vs denuder length L at 5, 10 and 20 L min^{-1} in indoor air (squares) and environmental tobacco smoke (triangles Δ), compared to predictions of the Possanzini model, Equations 3 and 4. C_o is the sum of the concentrations of phenanthrene collected on each of the three denuder sections. C for one denuder section (L=18.5 cm) is C_o - the sum of the concentrations found on the second and third sections. C for two denuder sections (L=37 cm) is the concentration found on the third denuder.

Figure 6. Particulate fractions of several semi-volatile PAH in ambient air in Berkeley, CA, over a 24-hr period in April 1995. Six IOVPS were used sequentially for 3.5 hr periods, every 4 hr, starting at 18:00 hr.

Figure 7. Gas-particle partitioning in Berkeley, CA, in April 1995. Arrhenius plots of -log K vs. $1000 \cdot T^{-1}$ where K is defined in Equation 6. F represents the PAH concentration in the particulate phase (filter + downstream denuder in ng m^{-3}), A is the gas phase concentration in the same units as F, and P is the mass concentration in μg m^{-3}.

Figure 8. Arrhenius plots (-log K vs $1000 \cdot T^{-1}$) for gas-particle partitioning in ETS over the temperature range 16-25°C. Data from five experiments: phenanthrene, circles o; pyrene, diamonds <>; and benz[a]anthracene, squares .

Figure 9. Gaseous (squares) and particulate (diamonds) concentrations of nicotine over a three hour period at 24 °C during and after the burning of three cigarettes by machine in a sealed 20 m^3 chamber with stainless steel walls.

Figure 10. The concentration of gas phase nicotine as a function of time after smoking for the experiment shown in Figure 9, as determined from the IOVPS and small co-located XAD-4 sorbent tubes. Just after the fifth IOVPS sample was collected, the chamber was vented for two hours, then resealed for three hours. During the last hour a final sorbent sample was collected to assess re-emission of nicotine from the walls.

Figure 11. Schematic diagram of the hybrid Integrated Organic Gas and Particle Sampler (IOGAPS). The glass tubes of the Gas and Particle (GAP) Sampler were stripped of their Tenax-silicone gum coating, sandblasted and recoated with ground XAD-4.

Figure 12. Schematic diagram of the prototype jumbo IOGAPS.

Table I. Comparison of surface characteristics of ground and unground XAD-4 resin

	Diameter μm	Surface Area $4\pi r^2$, cm^2	Volume $4/3\pi r^3$, cm^3	Surface/Volume cm^{-1}	Ground/Unground
Unground	760	0.018	2.3×10^{-4}	79	1015
Ground[a]	0.75[b]	1.8×10^{-8}	2.2×10^{-13}	8.0×10^{4}	

[a]Ground with a centrifugal ball mill.
[b]Geometric mean diameter as measured from electron photomicrographs (Figure 2).

Table II. Design parameters for three Integrated Organic Vapor/Particle Samplers. The predicted fraction of outlet to inlet gas phase conentrations for one denuder section, C/C_o, is illustrated for phenanthrene at 25°C.

Annulus Outer Diameter[a]	Annulus Width	Coated Length	Coated Area	Annular Volume[b]	Flow Rate	Reynolds Number	Face Velocity[c]	Transit Time[d]	Possanzini Eqn 3
d_2	d_2-d_1	L	A	V	F	Re	v	τ	C/C_o
cm	cm	cm	cm^2	cm^3	L min^{-1}		cm sec^{-1}	sec	
Single Channel									
2.4	0.1	18.5[e]	267	13.4	5	152	8.7	0.16	0.0022
					10	303	17	0.080	0.043
					20	607	35	0.040	0.19
					30	910	52	0.027	0.23
Four Channels[f]									
1.9	0.1	21.5[g]	567	28.4	5	83	8.7	0.34	2.9×10^{-6}
					10	166	17	0.17	1.5×10^{-3}
					20	332	35	0.085	0.036
					30	499	52	0.057	0.10
Five Channel[h]									
2.4	0.1	37.5[i]	1532	76.4	5	54	8.7	0.92	1.6×10^{-15}
					10	107	17	0.46	3.7×10^{-8}
					20	215	35	0.23	1.7×10^{-4}
					30	322	52	0.15	2.9×10^{-3}

[a]For the annulus with the largest outer diameter
[b]For the coated region only
[c]For filter exposed area of 9.62 cm^2 (47 mm diameter filter)
[d]Through coated length only
[e]Total length = 22 cm
[f]References 17 and 18
[g]Total length = 24 cm
[h]References 17-27
[i]Total length = 40 cm

Table III. Comparison of the single channel IOVPS to a filter-sorbent bed sampler for collection of gas-phase PAH in indoor air at two flow rates.[a]

PAH	Uncertainty %	Denuder/Sorbent ratio 10 L min^{-1}	Denuder/Sorbent ratio 20 L min^{-1}
Naphthalene	11.0	0.83±0.09	0.68±0.07
1- Methylnaphthalene	11.7	1.11±0.13	0.80±0.09
2- Methylnaphthalene	11.7	1.03±0.12	0.70±0.08
Biphenyl	22.7	1.03±0.23	0.60±0.13
Acenaphthene and acenaphthylene	14.0	0.87±0.12	0.72±0.10
Fluorene	30.4	0.95±0.29	0.85±0.26
Phenanthrene	14.5	1.18±0.17	0.94±0.14
Anthracene	12.7	0.94±0.12	0.95±0.12
Fluoranthene	12.7	1.00±0.13	0.84±0.11
Pyrene	29.6	1.05±0.31	0.84±0.25
Average (All PAH)		1.00±0.10[b]	0.79±0.11[b]

[a] Three-hour sampling periods on two different days. The configurations of Figure 4b and Figure 4a were used for sampling at 10 and 20 L min^{-1}, respectively. Uncertainty estimate is based on propagation of errors using the relative precision data of Reference 14.

[b] Standard deviation derived from the average of denuder/sorbent ratios.

Table IV. Phase distributions of polycyclic aromatic hydrocarbons in indoor laboratory room air at 21°C for co-located IOVPS and filter-sorbent bed samplers at 20 L min^{-1} for 3 hr.[a]

PAH	IOVPS (g) ng m^{-3}	IOVPS (p)[b] ng m^{-3}	IOVPS $p\cdot(g+p)^{-1}$	Filt-Sorb (g) ng m^{-3}	Filt-Sorb (p) ng m^{-3}	Filt-Sorb $p\cdot(g+p)^{-1}$
Phenanthrene	39.1±4.0	3.43±0.37	0.08±0.02	41.5±4.3	1.42±0.15	0.03±.01
Pyrene	2.42±0.51	0.44±0.08	0.15±0.07	2.88±0.60	0.17±0.03	0.06±0.03

[a] Uncertainties are based on propagation of errors, using the relative precision data of Reference 14.

[b] No post-filter denuder or sorbent was used, so amounts of PAH desorbed from the post-denuder filter were unknown.

Table V. Phase distributions of polycyclic aromatic hydrocarbons in simulated environmental tobacco smoke at 16 °C.[a]

PAH	gas ng m^{-3}	particles ng m^{-3}	fraction in particles[b]
Naphthalene	822±102	<17	<0.02
1-Methylnaphthalene	334±23	<12	<0.04
2-Methylnaphthalene	526±50	<10	<0.02
Acenaphthene and acenaphthylene	72.2±15.1	<1.4	<0.02
Fluorene	56.5±4.4	<1.7	<0.02
Phenanthrene	43.1±11.5	<5.2	<0.11
Anthracene	3.85±0.67	<0.1	<0.03
Fluoranthene	3.73±0.66	2.3±0.9	0.38±0.08
Pyrene	13.8±5.3	3.0±0.4	0.18±0.10
Benz[a]anthracene	0.15±0.04	10.4±0.5	0.99±0.28
Chrysene	0.86±0.09	30.1±4.4	0.97±0.28

[a] Sampled at 5 L min^{-1} for 1 hour. Uncertainties are the standard deviations derived from the data of Reference 14.

[b] Uncertainties are estimated from propagation of errors using the standard deviations.

Table VI. Design parameters for high capacity Integrated Organic Gas and Particle Samplers. The predicted fraction of outlet to inlet gas phase concentrations for one denuder section, C/C_o, is illustrated for phenanthrene at 25°C.

Annulus Outer Diameter[a]	Annulus Width	Coated Length	Coated Area	Annular Volume[b]	Flow Rate	Reynolds Number[c]	Face Velocity[d]	Transit time[e]	Possanzini Eqn 3[c]
d_2	d_2-d_1	L	A	V	F	Re	v	τ	C/C_o
cm	cm	cm	cm^2	cm^3	L min^{-1}		cm sec^{-1}	sec	
Hybrid IOGAPS									
5.1	0.15-0.30	60	6151	717	16.7	92	29	2.6	5.2×10^{-5}
					30	165	52	1.4	3.8×10^{-3}
					50	275	87	0.86	3.3×10^{-2}
					75	413	130	0.57	9.5×10^{-2}
IOGAPS									
4.8	0.10-0.14	58[f]	6990	400	16.7	74	29	1.4	1.5×10^{-12}
					30	133	52	0.80	2.4×10^{-7}
					50	222	87	0.48	9.8×10^{-5}
					75	334	130	0.32	2.0×10^{-5}
Jumbo IOGAPS[g]									
4.8	0.10-0.14	58[f]	6990	400	30	133	17	0.80	2.4×10^{-7}
					50	222	29	0.48	9.8×10^{-5}
					75	334	43	0.32	2.0×10^{-5}
					100	445	57	0.24	8.9×10^{-3}
					125	556	72	0.19	2.2×10^{-3}

[a]For the annulus with the largest outer diameter
[b]For the coated region only
[c]For widest annulus
[d]For filter exposed area of 9.6 cm^2 (47 mm diameter filter) for the Hybrid IOGAPS and IOGAPS; exposed filter area of 29 cm^2 for the Jumbo IOGAPS
[e]Through coated length only
[f]Total length = 60 cm
[g]For one denuder section; the jumbo-IOGAPS incorporates two parallel denuder-filter-PUF (PS-1) samplers for total flow rate and capacity double the values listed here.

Table VII. Comparison of diffusion denuder and conventional sampling of ambient PAH (April 1995, Berkeley, California, USA).

	IOVPS[a]			Hybrid IOGAPS[b, c]			Filter-Sorbent Sampler[d]		
ng m^{-3}	Gas[e]	Particles	Total	Gas[f]	Particles	Total	Gas[f]	Particles	Total
Naphthalene	244	1.6	245	285	38	323	444	0.023	444
1-Methylnaphthalene	61	0.6	62	87	1.9	89	102	0.009	102
2-Methylnaphthalene	111	3.8	115	154	2.2	156	176	0.008	176
Phenanthrene	8.4	-[g]	>8.4	-[g]	0.89	>0.89	8.4	0.036	8.4
Anthracene	0.29	0.04	0.32	0.11	0.03	0.14	0.52	0.001	0.52
Fluoranthene	1.6	0.49	2.1	0.6	0.8	1.4	1.8	0.030	1.8
Pyrene	1.6	0.62	2.2	1.8	0.25	2.1	1.7	0.052	1.7
Benz(a)anthracene	0.16	0.12	0.28	-[g]	0.18	>0.18	0.04	0.033	0.070
Chrysene	0.11	0.19	0.31	-[h]	0.13	>0.13	0.43	-[h]	>0.43

[a] Six IOVPS operated sequentially for 3.5 hr periods at 10 L min^{-1}.

[b] IOGAPS operated for 24 hr at 16.7 L min^{-1}. Total mass of particles (<10 mm) = 16.7 mg m^{-3}.

[c] Concentrations of high molecular weight PAH from IOGAPS: benzo(b)fluoranthene, 31; benzo(k)fluoranthene, 16; benzo(a)pyrene, 25; benzo(ghi)perylene, 47 pg m^{-3}; from conventional sampler: benzo(b)fluoranthene, 39; benzo(k)fluoranthene, 16; benzo(a)pyrene, 27; benzo(ghi)perylene, 52 pg m^{-3}.

[d] Filter-sorbent sampler operated for 24 hr at 16.7 L min^{-1}. Total mass of particles (<10 mm) = 16.9 mg m^{-3}.

[e] For the naphthalenes only, the 20 hr average (5 IOVPS) is given, excluding the last sampling period, because these compounds were lost during evaporation of the 6th period extract.

[f] Data for naphthalenes include self-absorption corrections to fluorescence data; estimated uncertainty, 20%.

[g] High blank.

[h] Not measured

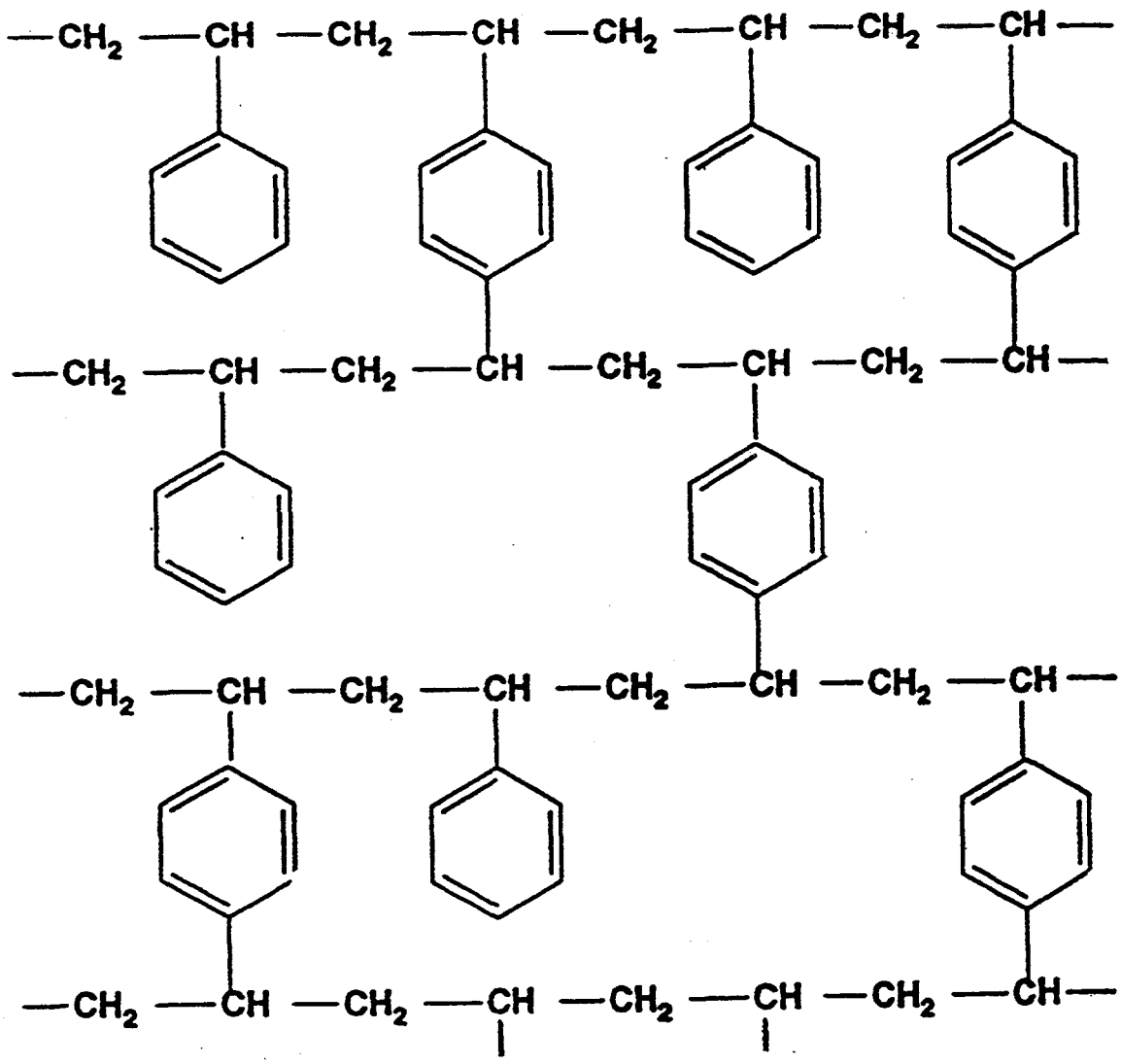

Figure 1. The chemical structure of styrene-divinylbenzene copolymer macroreticular resins such as XAD-2, XAD-4, XAD-16, Chromosorb 102 and Ostion SP-1. Adapted from US Patent 4,224,415, R.M. Patel et al., American Laboratory, Feb. 1990, and G.A. Junk, Symposium on Solid Phase Extraction, American Chemical Society, 205th Annual Meeting, San Francisco, Mar. 28-Apr. 2, 1992.

Figure 2. Scanning electron photomicrographs of (top) an uncoated sandblasted glass annular denuder fragment, and (bottom) an annular denuder fragment coated with ground XAD-4 adsorbent. The instrument was operated at 20 keV, 50 μm beam, 26° tilt and 12-mm working distance.

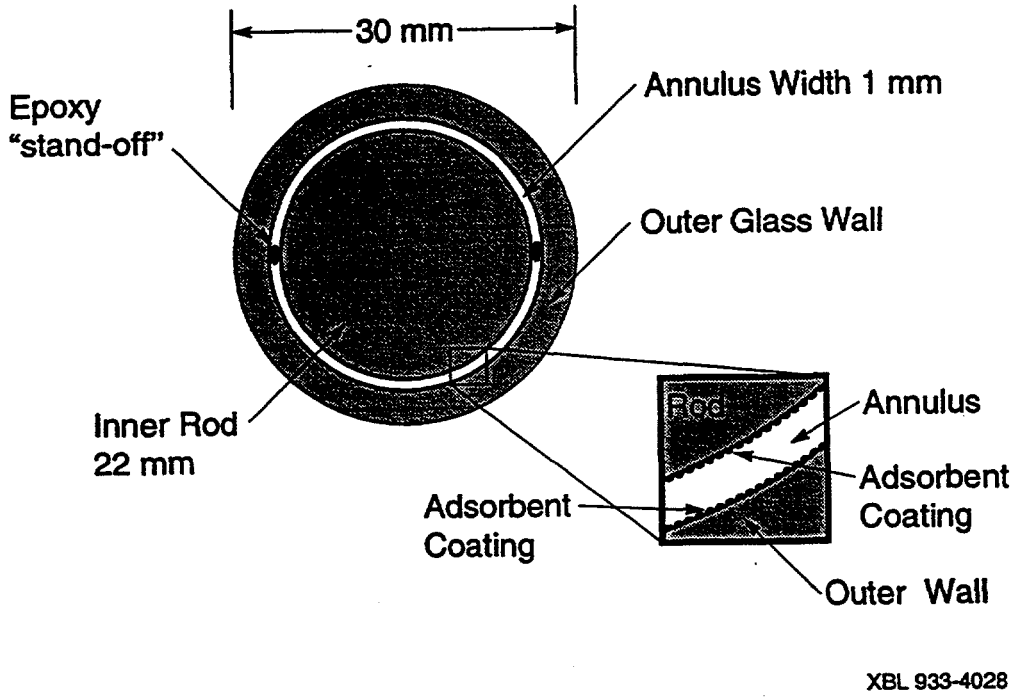

Figure 3. Cross section of a single channel coated annular denuder. The dimesions shown apply to the Integrated Organic Vapor/Particle Sampler (IOVPS).

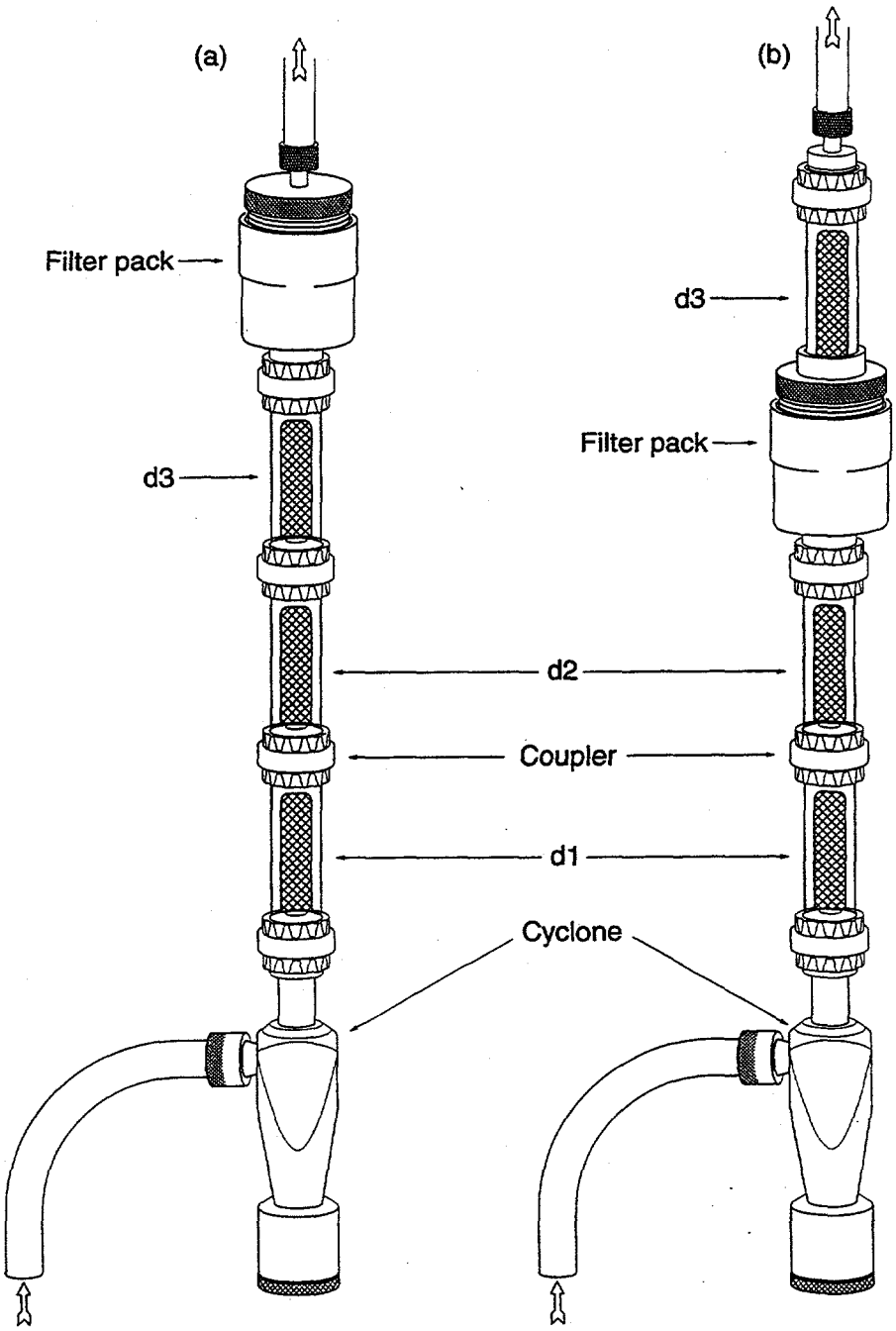

Figure 4. Sampling configurations for the IOVPS. The arrows show the direction of airflow. d1, d2 and d3 indicate XAD-4 coated glass annular denuder sections, each with coated length of 18.5 cm, that are connected by threaded couplers. Cross-sectional dimensions are shown in Figure 3. The filter pack holds one or two 47-mm diameter filters. (a) The configuration used for initial testing and validation studies in combustion-free indoor air. (b) The configuration used for sampling simulated environmental tobacco smoke in an environmental chamber. This configuration was also used for phase distribution measurements in outdoor ambient air.

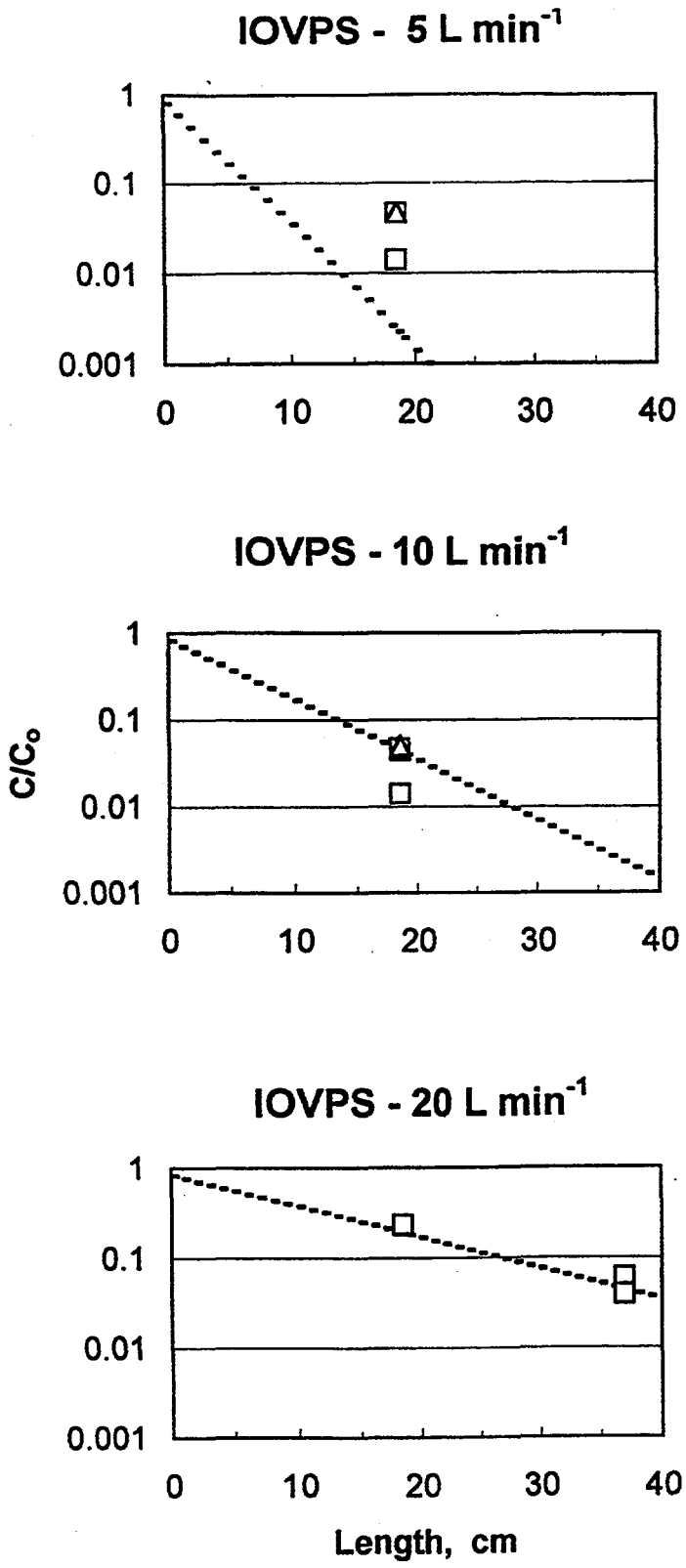

Figure 5. The ratio of outlet concentration phenanthrene C to inlet concentration C_o vs. denuder length L at 5, 10 and 20 L min^{-1} in indoor air (squares) and environmental tobacco smoke (triangles Δ), compared to predictions of the Possanzini model, Equations 3 and 4. C_o is the sum of the concentrations of phenanthrene collected on each of the three denuder sections. C is the sum of the concentrations of phenanthrene collected on each of the three denuder sections. C for one denuder section (L=18.5 cm) is C_o - the sum of the concentrations found on the second and third sections. C for two denuder sections (L=37 cm) is the concentration found on the third denuder.

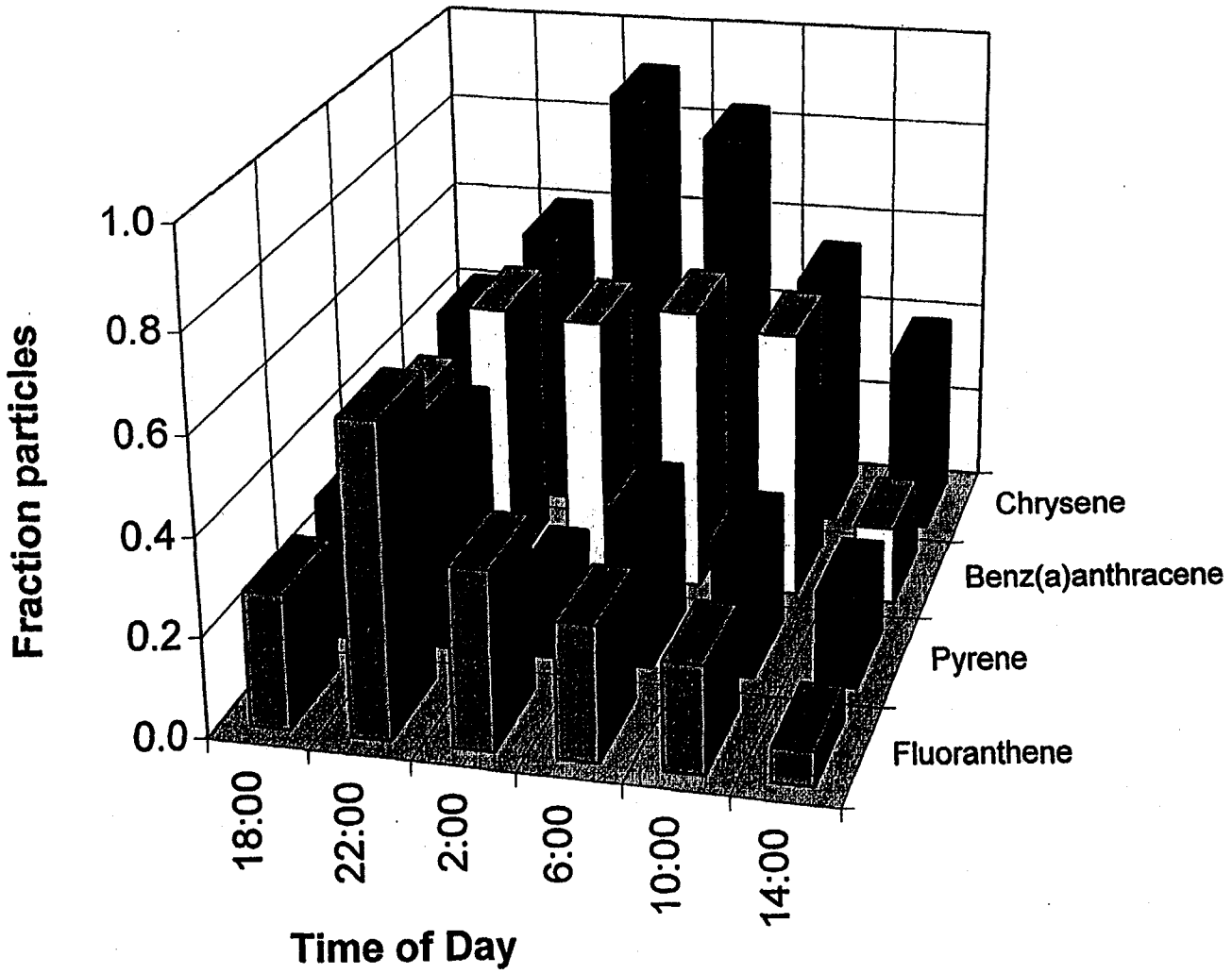

Figure 6. Particulate fractions of severalsemi-volatile PAH in ambient air in Berkeley, CA, over a 24-hr period in April, 1995. Six IOVPS were used sequentially for 3.5 hr periods, every 4 hr, starting at 18:00 hr.

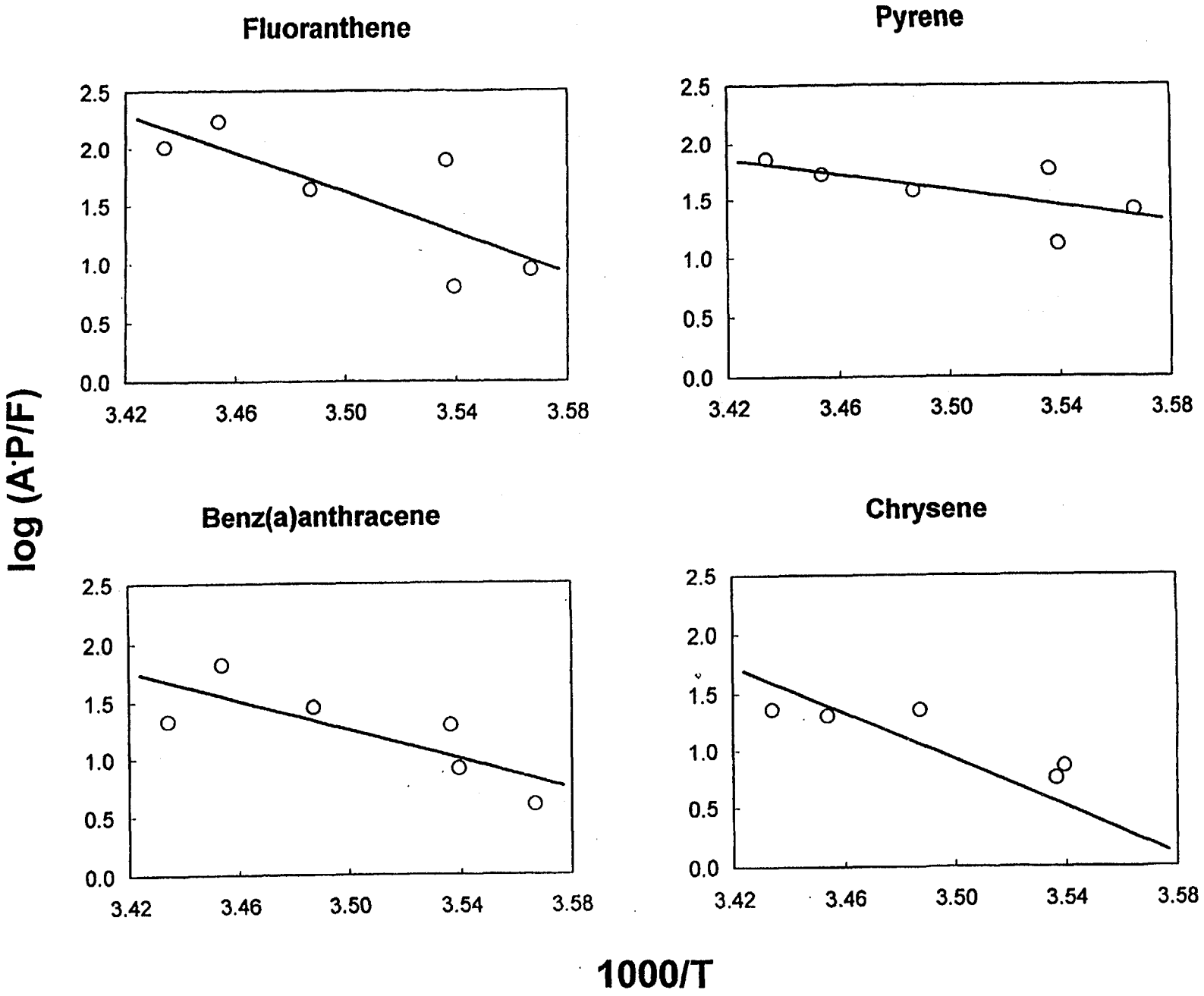

Figure 7. Gas-particle partitioning in Berkeley, CA, in April 1995. Arrhenius plots of -log K vs. 100 T^{-1} where K is defined in Equation 6. F represents the PAH in the particulate phase (filter + downstream denuder in ng m^{-3}), A is the gas phase concentration in the same units as F, and P is the mass concentration in μ g m^{-3}.

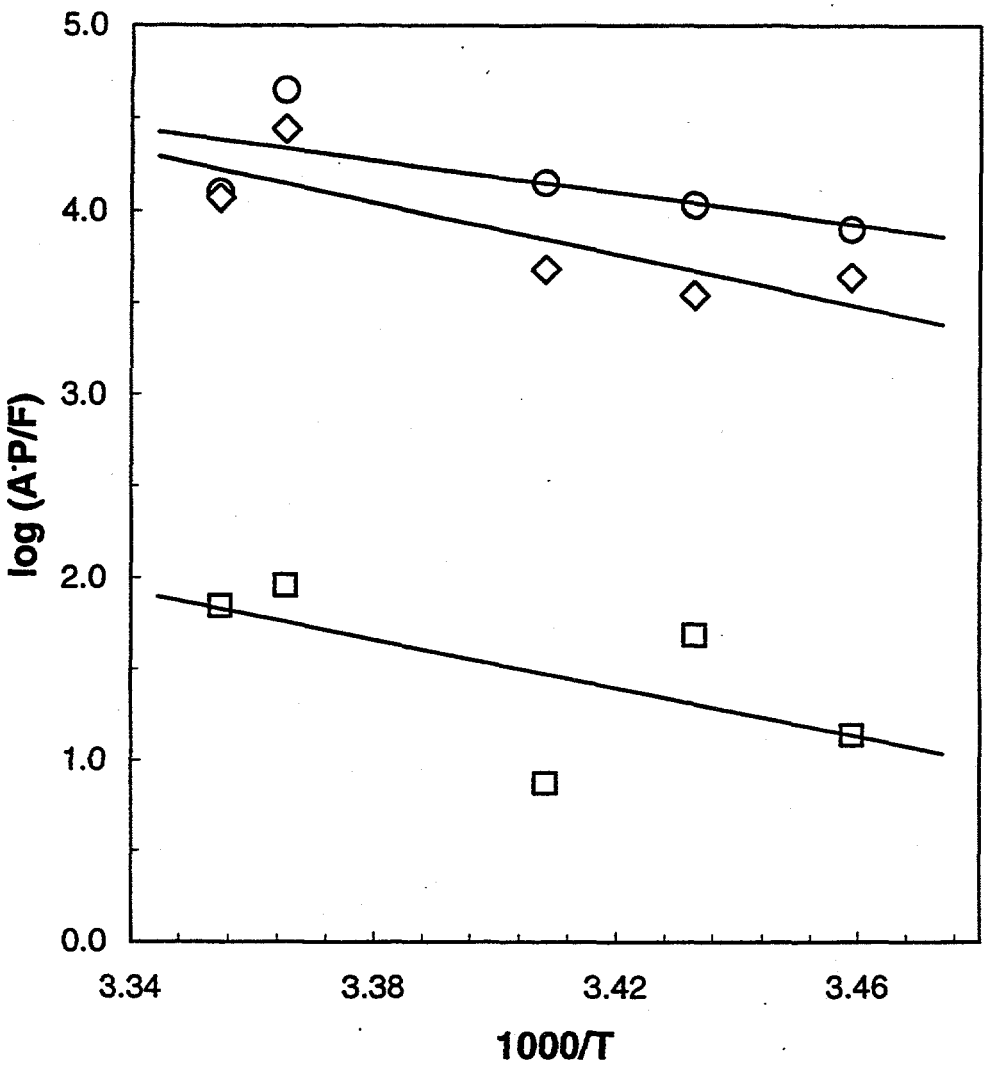

Figure 8. Arrhenius plots (- log K vs. 100-T^{-1}) for gas-particle partitioning in ETS over the temperature range 16-25°C. Data from five experiments: phenanthrene, circles 0; pyrene, diamonds <>; and benz [a] anthracene, squares.

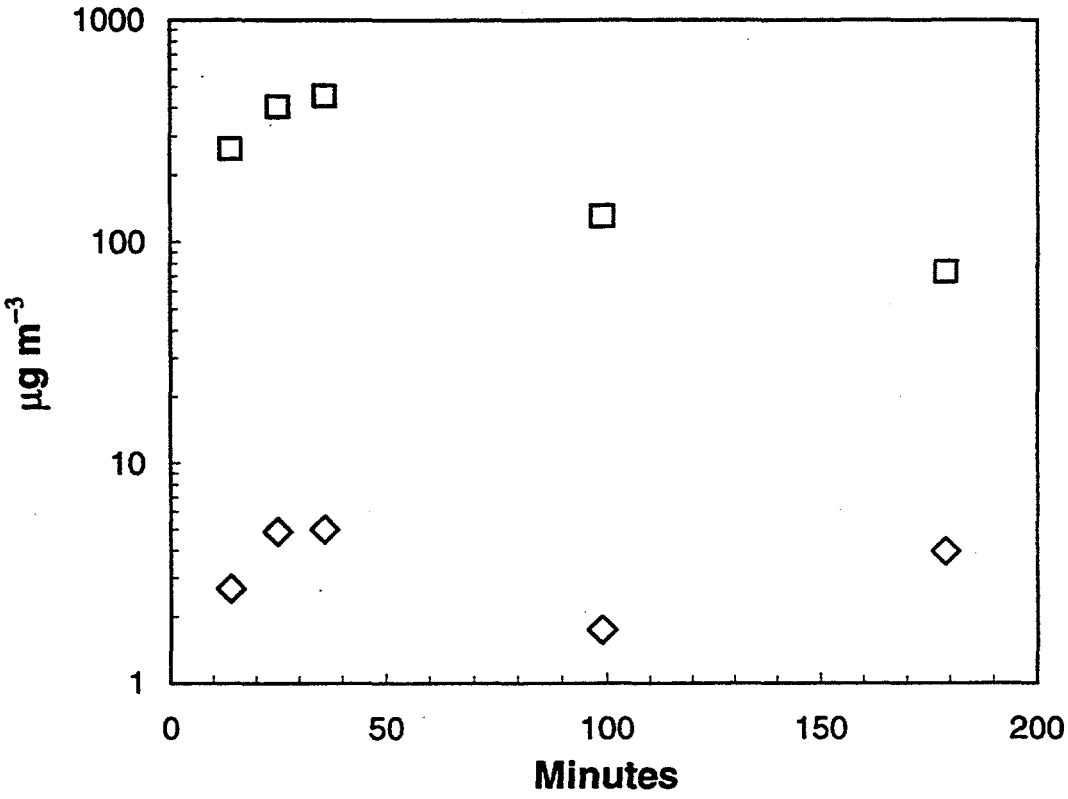

Figure 9. Gaseous (squares) and particulate (diamonds) concentrations of nicotine over a three hour period at 24° C during and after the burning of three cigarettes by machine in a sealed 20 m^3 chamber with stainless steel walls.

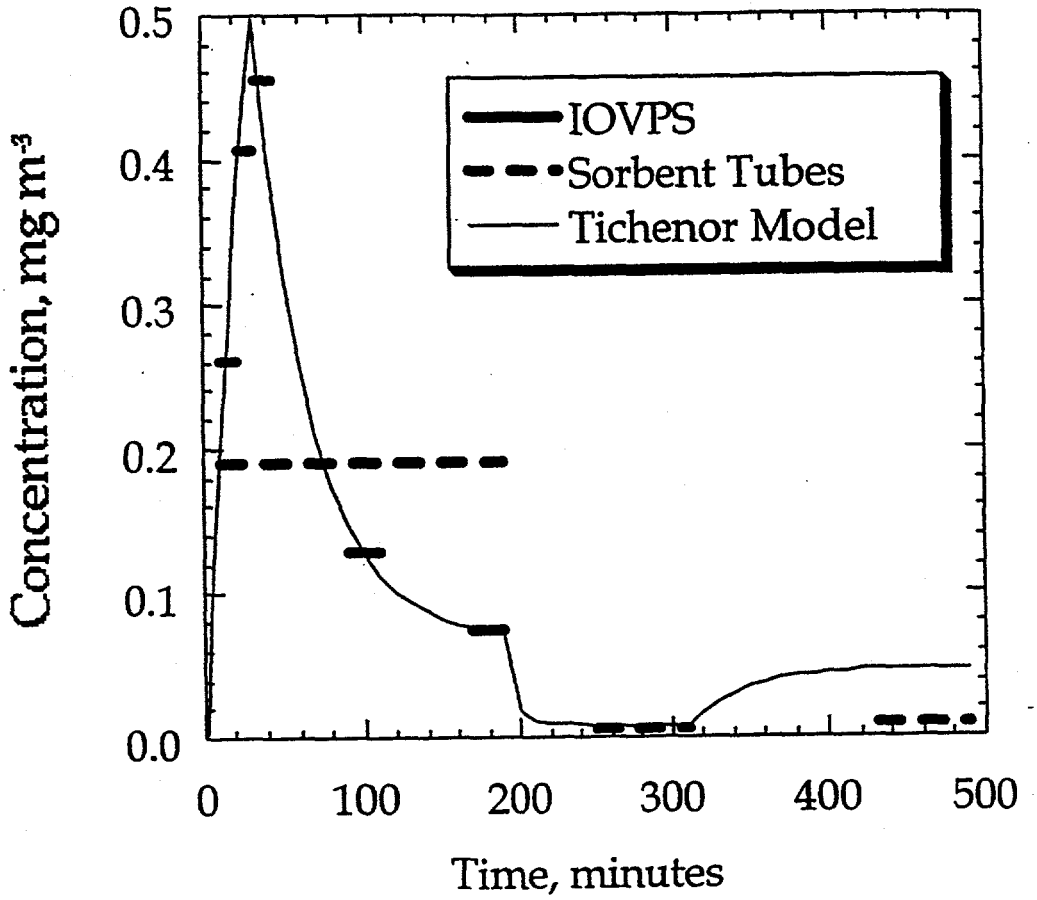

Figure 10. The concentration of gas phase nicotine as a function of time after smoking for the experiment shown in figure 9, as determined from the IOVPS and small co-located XAD-4 sorbent tubes. Just after the fifth IOVPS sample was collected, the chamber was vented for two hours, then resealed for three hours. During the last hour a final sorbent sample was collected to assess re-emission of nicotine from the walls.

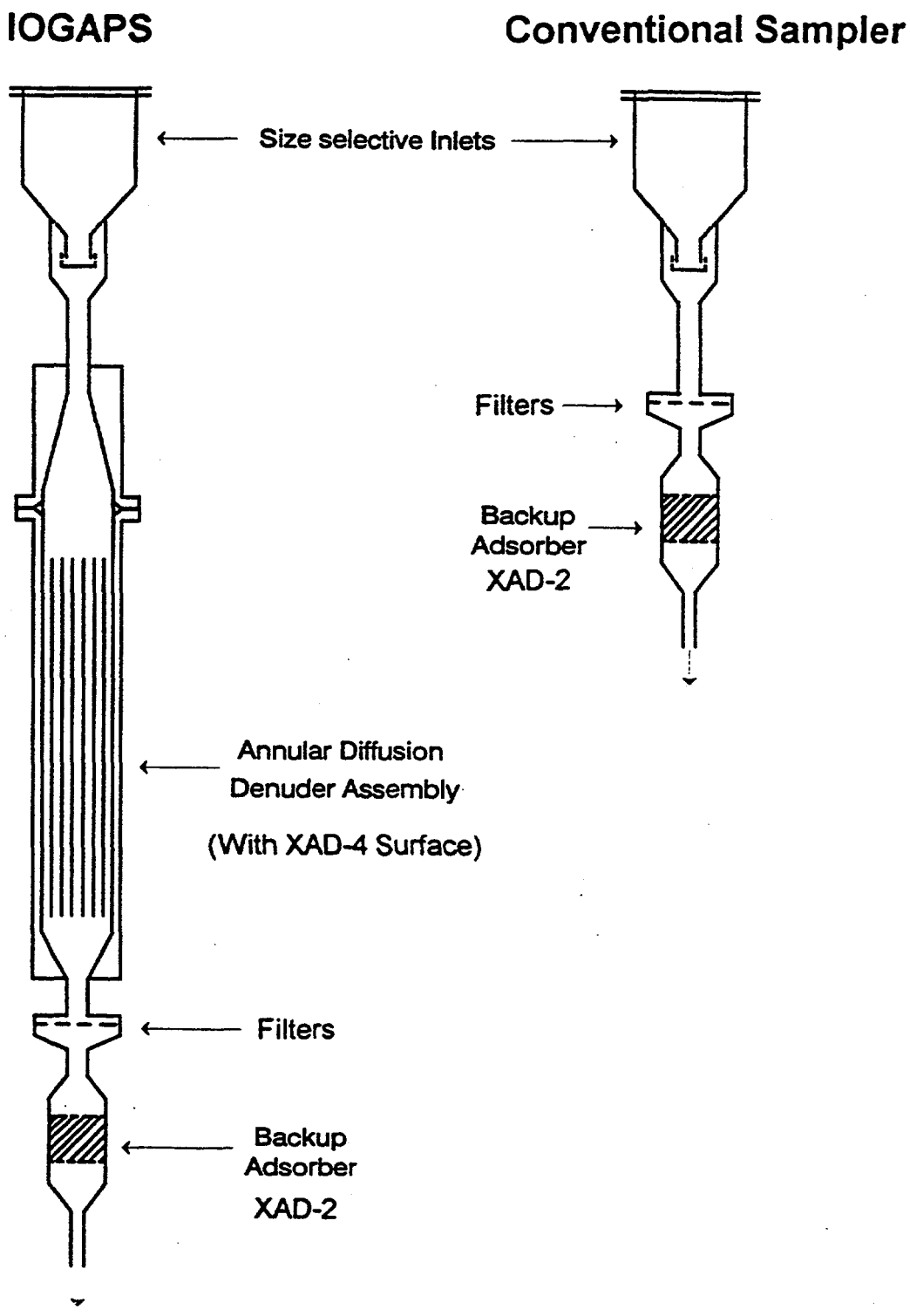

Figure 11. Schematic diagram of the hybrid Integrated Organic Gas and Particle Sampler (IOGAPS). The glass tubes of the Gas and Particle (GAP) Sampler were stripped of their tenax-silicone gum coating, sandblasted and recoated with ground XAD-4.

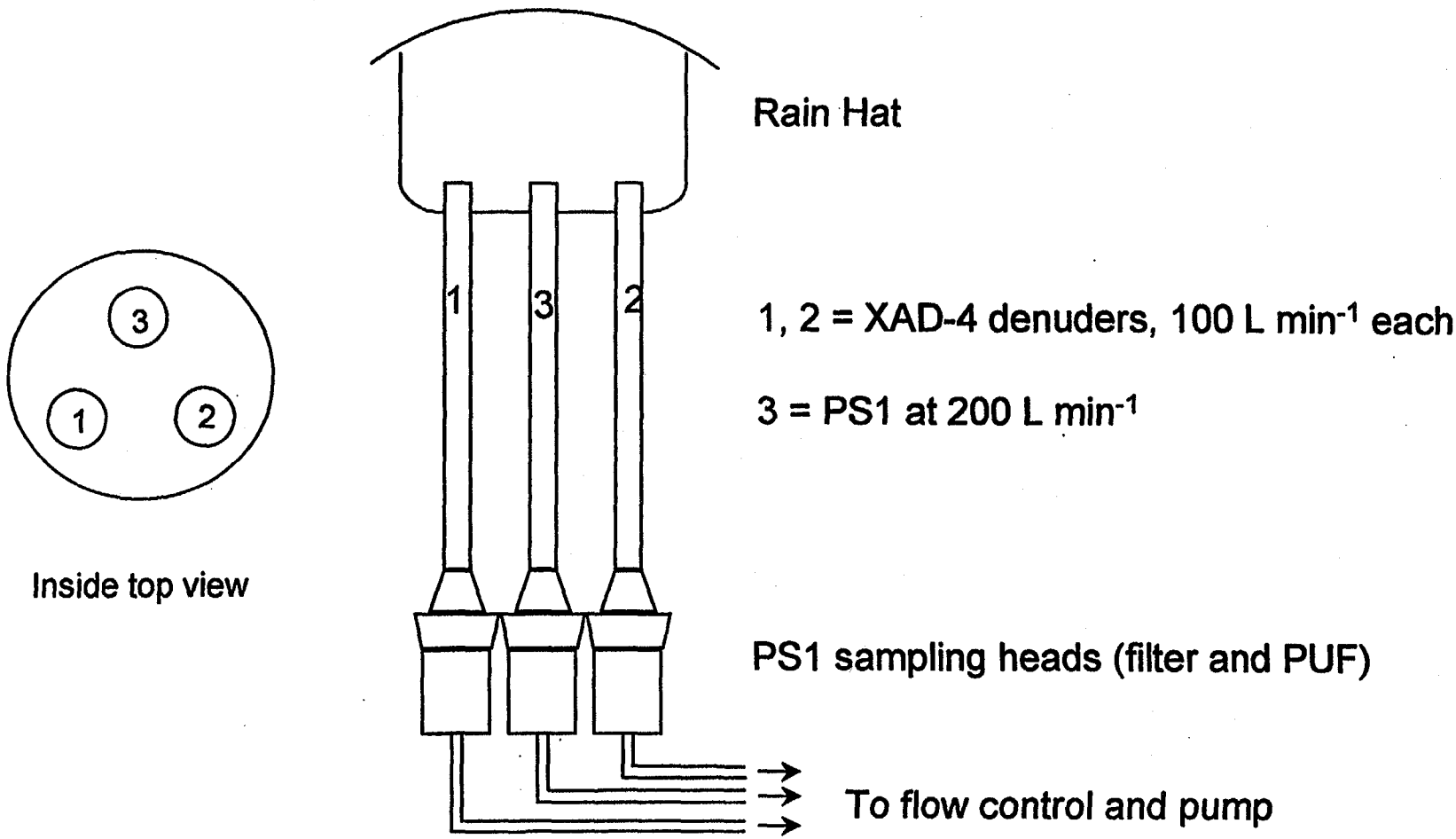

Figure 12. Schematic diagram of the prototype jumbo IOGAPS.